LONGITUDINAL MESOSCALE CALCIUM IMAGING OF REGIONAL ACTIVITY AND INTER-REGIONAL CONNECTIVITY AFTER ELECTROCONVULSIVE STIMULATION

by

D. Blair Jovellar

A THESIS SUBMITTED IN PARTIAL FULFILLMENT OF
THE REQUIREMENTS FOR THE DEGREE OF

MASTER OF SCIENCE

in

THE FACULTY OF GRADUATE AND POSTDOCTORAL STUDIES
(Neuroscience)

THE UNIVERSITY OF BRTISIH COLUMBIA
(Vancouver)

November 2018

The following individuals certify that they have read, and recommend to the Faculty of Graduate and Postdoctoral Studies for acceptance, a thesis/dissertation entitled:

Longitudinal mesoscale calcium imaging of regional activity and inter-regional connectivity after electroconvulsive stimulation

submitted by Desiree Blair A. Jovellar in partial fulfillment of the requirements for

the degree of MSc.

in Neuroscience

Examining Committee:

Timothy H. Murphy, PhD
Supervisor

Victor Viau, PhD
Supervisory Committee Member

Fidel Vila-Rodtriguez, MD
Supervisory Committee Member

Doris J. Doudet, PhD
Additional Examiner

Additional Supervisory Committee Members:

Yutian Wang, PhD
Supervisory Committee Member

ABSTRACT

Introduction

Depression is a leading cause of disability worldwide. As a treatment for depression, electroconvulsive therapy (ECT) remains the most effective. In spite of such unparalleled efficacy, our understanding of the therapeutic mechanisms of ECT remains lacking. Using Electroconvulsive stimulation (ECS)—an animal model of ECT—we determine acute and chronic changes in functional connectivity and frequency-specific modulation after ECT.

Methods

Wide-field fluorescent imaging of resting-state activity was performed in awake head-fixed mice expressing GCaMP6 (a genetically-encoded calcium indicator). GCaMP allows longitudinal imaging of intracellular calcium dynamics while wide-field imaging at a mesoscale captures neuronal population activity across brain regions. ECS was done once daily, every other day, for a total of 10 treatments. Imaging was done daily 5-10 min and 24h after ECS. Sham animals were handled similar to ECS animals, including application of auricular electrodes, without electrical stimulation.

Results

Quantification of GCaMP6 fluorescence reveals time-dependent changes in functional connectivity after ECS. The acute post-stimulation period reveals a widescale increase in functional connectivity, which is remarkably reversed 24h after. Further graph theoretical analysis demonstrates that the primary motor (M1) area has the highest increase in total strength of connections (i.e., node strength) acutely after stimulation while the retrosplenial cortex (RS)

shows the greatest decrease in node strength after 24h. Moreover, spectral analysis shows that ECS results in increased power in delta and theta bands together with a decrease in alpha. These frequency-dependent changes are region-specific.

Conclusions

The changes in power in delta, theta, and alpha bands indicate that ECS induces region-specific slowing of activity within cortical regions. Previous work demonstrates that in the approach to seizure termination, brain electrical activity exhibits the following dynamical signatures: increased temporal correlation and decreased dominant oscillation frequency. The highest increase in connectivity strength in M1 together with slowing of oscillation frequency acutely after ECS suggests that M1 plays a role in seizure termination. The significant decrease in connectivity strength in RS, together with slowing of oscillations 24h after ECS may indicate that RS mediates both therapeutic (ie., antidepressant) and adverse cognitive effects (i.e., memory loss) after ECT.

LAY SUMMARY

Using Electroconvulsive stimulation (ECS)—an animal model of ECT—we determine acute and chronic changes in the co-activation of different brain regions and how the rate at which regional brain activity fluctuates (i.e., frequency), using a mouse model. ECS was done once daily, every other day, for a total of 10 treatments. Imaging was done daily 5-10 min and 24h after ECS.

We found that the correlated activity between brain regions increased right after ECS and decreased 24h after. Right after stimulation, the primary motor cortex (M1) shows a significant increase in correlated activity with all other regions while 24h after, the retrosplenial cortex (RS) shows a significant decrease in co-activation with all other regions. We also found that ECS increases the rate at which regional brain activity fluctuates (i.e., frequency) in slower frequency bands (delta and theta) and decreases activity in the higher alpha frequency band.

PREFACE

All experimental protocols were approved by the animal care committee in the University of British Columbia and all procedures were followed with strict compliance in accordance to guidelines provided by the Canadian Council for Animal Care. The animal protocol of relevance is A18-0036-A004.

Data presented in this study are results of experiments performed in the lab of Dr. Tim H. Murphy, in the University of British Columbia. I designed the study, which was approved by Dr. Murphy. Animal surgeries were done by Mr. Pumin Wang and myself. I performed all stimulation and imaging experiments, as well as data analysis. Original MATLAB codes were provided by Dr. Matthieu Vanni and Mr. Jeffrey LeDue. These were edited by Mr. LeDue and myself. I also built the head-fixation apparatus, ECS stimulation chamber, and imaging chamber, with guidance from Mr. LeDue on assembly of LEDs for imaging.

I was responsible for writing this thesis, including generating all figures, with comments from Dr. Tim H. Murphy and Dr. Doris J. Doudet.

TABLE OF CONTENTS

List of Figures

List of Abbreviations

BC Barrel Cortex
ECS Electroconvulsive stimulation
ECT Electroconvulsive therapy
FL Forelimb somatosensory cortex
FMRI Functional Magnetic Resonance Imaging
GECI Genetically Encoded Calcium Indicator
HL Hindlimb somatosensory cortex
LFP Local Field Potential
M1 Primary Motor Cortex
M2 Secondary Motor Cortex
PT Parietal Cortex
ROI Region of Interest
RS Retrosplenial Cortex
SPC Seed Pixel Correlation

ACKNOWLEDGEMENTS

Firstly, I thank my supervisor, **Dr. Timothy H. Murphy**, for providing me with support and the opportunity to pursue this project. Establishing the ECS protocol in GCaMP6 mice was no easy feat and Dr. Murphy's patience and feedback helped me push through until the end.

I am deeply grateful to **Dr. Matthieu P. Vanni** for his mentorship throughout my stay in the lab and beyond. Aside from technical discussions, his guidance, moral support, and positivity fostered my growth as a researcher and as an individual.

Dr. Doris J. Doudet has been a great inspiration—scientifically and personally. The opportunities she provided me in research and teaching are above and beyond what is expected—and for that, I express my deep gratitude. Her guidance, voice of reason, and motivation are truly inestimable.

Dr. Shernaz X. Bamji opened the door for me to the world of neuroscience. I am grateful that she saw my potential early on and developed it. I truly appreciate her trust for letting me contribute to three projects during my stay in her lab.

I appreciate the insightful comments and suggestions by my supervisory committee and examiners (in addition to Dr. Murphy and Dr. Doudet): **Dr. Victor Viau, Dr. Yutian Wang, Dr. Fidel Vila-Rodriguez**. A special thank you to **Dr. Vila-Rodriguez** for also providing support and for introducing me to brain stimulation therapies (TMS, ECT, and ECS).

I am tremendously grateful to **Mr. Jeffrey LeDue** for his patience, guidance, and direct contributions to MATLAB analysis and helping me set-up the three-colour LEDs for GCaMP imaging. The technical discussions, moral support, and positive attitude he shared are invaluable.

I acknowledge **Mr. Pumin Wang** for training me in rodent surgical techniques and for the chronic window surgeries he has done. I also thank **Dr. Catalin Mitelut and Mr. Dirk Haupt** for providing Python codes for Raspberry PiCam imaging and for their friendship.

All of this would not be possible without the love and support of my friends and especially my family. I express my deepest gratitude to my parents **Atty. Alejandro Jovellar and Mrs. Adoracion Jovellar,** for being my rock throughout the years and for supporting me in achieving my goals and aspirations.

To Al and Sionnie,
for being the epitome of grit, integrity, and kindness,
and for engendering in us to dream the impossible dream

EPIGRAPH

"Only the free mind can discover. You cannot discover the truth of anything by merely being told what it is, because then the discovery is not yours….

Work patiently at your studies, not that men may think you are wise, not even that you may have the happiness of being wise, but because only the wise man can be wisely helpful."

- J. Krishnamurti

Chapter 1: INTRODUCTION

Depression is a leading cause of disability worldwide (WHO, 2018) and one in six people experience depression in their lifetime (Kessler et al., 2005). This disorder has been linked to imbalanced communication between neural networks in the brain (Kaiser et al., 2015; Khalid et al., 2014). Electroconvulsive therapy (ECT) prevails as the most effective treatment for depression with a response rate of 70% to 85.7% (Brakemeier et al., 2013 and Tokutsu et al., 2013). In spite of such unparalleled efficacy, our understanding of the mechanism of the therapeutic and memory side effects of ECT remains lacking.

I have established an ECT model in the lab with parameters simulating human ECT in mice. ECT employs electrical stimulation to induce seizures in a controlled environment. Using transgenic mice with genetically encoded indicators of cellular activity in the brain (i.e., GCaMP6), we can track changes in regional activity and inter-region correlated activity longitudinally. This is an excellent tool to examine regional and network changes induced by neuropsychiatric diseases—which are typically chronic disorders.

Recent work in our lab demonstrates a wide-scale increase in functional connectivity in a mouse model of depression. As such, our central hypothesis is that ECT acts to correct aberrant hyperconnectivity observed in neuropsychiatric disorders such as major depression. The overall goal of this project is to examine how neuronal networks change after ECT—emphasizing effects on brain regions that are also relevant to ECT-induced memory loss. Impairment of episodic memory is the most prominent side effect of ECT. Elucidating the changes in regional activity and inter-region connectivity may provide insights on the mechanism of memory loss as well as the therapeutic mechanism of ECT.

1.1. Electroconvulsive stimulation (ECS) as an Electroconvulsive therapy (ECT) model

1.1.1. Electroconvulsive therapy (ECT): Origin and development

The inception of electroconvulsive therapy was spearheaded by Ugo Cerletti and Luigi Bini in 1938 when they demonstrated ECT in Rome for the first time (Cerletti and Bini, 1938). ECT—the application of electrical stimulation on the scalp to induce generalized seizures with the goal of alleviating psychiatric symptoms—has undergone a number of technical and operational modifications since then (Leiknes et al., 2012). Originally, Cerletti and Bini used bitemporal placement of electrodes and applied 120V sine-wave electrical current to the head (Cerletti and Bini, 1938). Technical advances include the development of square wave, brief-pulse electrical current devices. Operationally, modifications include change in the location of electrode placement—bifrontal and right unilateral (in addition to bitemporal)—and the use of anesthesia and muscle relaxant during stimulation.

Historically, ECT was administered without anesthesia, subsequently it was deemed necessary to apply anesthetic and muscle relaxant (usually succinylcholine) during stimulation. Doing so reduces side effects from convulsions such as bone fractures, dental and tongue injury, as well as damage to muscles and tendons (Leiknes et al., 2012). Modified ECT—with the application of anesthetic and muscle relaxant—has been the recommended protocol in the last decade according to internationally established guidelines (American Psychiatric Association 2001; Royal College of Psychiatrists 2005; Enns et al. 2010; Leiknes et al., 2012).

ECT electrode placement is a major determinant of the spatial distribution of induced electric field and relative degree of stimulation of different brain regions (Peterchev et al., 2010). When electrodes are close together, i.e., during right unilateral ECT, the maximum cortical electric field lies between the two electrodes (Peterchev et al., 2010), and increasing electrode proximity increases focality at the cost of more surface current (Datta et al., 2008)—resulting in more

current shunting across the scalp and weaker electric field in the brain (Peterchev et al., 2010). On the other hand, when electrodes are widely-spaced—ie., during bitemporal ECT—this results in diffuse modulation with bi-directional radial modulation under each electrode and tangential modulation between electrodes (Datta et al., 2008). The most intense seizure activity is seen in brain regions with the highest electrical current density (Swartz and Nelson, 2005). Alterations in electrode placement have been done in an effort to target specific structures that putatively confer therapeutic benefit while avoiding or minimizing involvement of regions that may contribute to side effects such as memory impairment.

The technical and operational modifications in ECT have been implemented to improve patient safety and to attenuate adverse effects while maintaining therapeutic benefit.

1.1.2. Clinical applications

Originally, ECT was used in the treatment of schizophrenia **(**Leiknes et al., 2012). In 1941, the efficacy of ECT for patients with depression and mania was established (Hemphill and Walter 1941). Nowadays, ECT is used worldwide as one of the most effective treatments for a number of severe, treatment-resistant disorders (Kerner and Prudic, 2014). As for current applications of ECT, it has been shown to improve response rates in drug-resistant disorders with depressive, manic, and catatonic states (Perugi et al, 2017, Baghai 2008, Gitlin, 2006). It also imparts clinical improvement in patients with schizoaffecgtive disorder (Gitlin, 2006) and especially depression with psychotic features (Rothschild, 2013, Baghai 2008, Petrides et al., 2001). ECT has also been shown to be effective in the fast symptomatic relief of suicidal ideation and behaviour. A study by Kellner et al., (2005) demonstrated absence of suicidal intent after the third treatment. Additionally, when depression, mania, and psychotic symptoms occur during pregnancy or the post-partum breastfeeding period whereby oral medications are precluded due

to systemic side effects, ECT remains a practicable first-line treatment option (Baghai and Moller, 2008). Aside from psychiatric disorders, ECT also provides clinical improvement in neurodegenerative disorders, particularly Parkinson's disease. In humans, ECT has been shown to improve motor performance (Kennedy et al., 2003) and ECS has also been demonstrated to enhance gross motor function in a rat model of Parkinson's diseases (Strome et al., 2007).

1.1.3. How ECT is applied in humans

The modern clinical application of ECT is a result of decades of research to improve patient safety and attenuate adverse effects while maintaining therapeutic benefit. In this section we discuss current stimulus parameters and contemporary practice of ECT.

Stimulus parameters

Stimulus parameters include waveform, pulse width, frequency, train duration, and amplitude. Brief pulse stimulus has replaced sine wave stimulus since 2001 as sine wave produced worse cognitive impairment than brief pulse stimulus (Kerner and Prudic, 2014). Sine wave currents consist of a continuous stream of electricity which flows in alternating directions (i.e., positive and negative). This continuous flow of current results in more electrical charge than is necessary to elicit a seizure (Andrade, 2010). On the other hand, brief pulse stimulus is characterized by rectangular pulses of current separated by brief periods without electrical activity. Pulse width refers to the duration of each pulse and is measured in milliseconds. Brief pulse stimulus has a pulse width of 0.5–2.0 milliseconds (Kerner and Prudic, 2014). The number of alternations between positive and negative current flow (number of cycles per second) is referred to as frequency—this ranges from 10-140 Hz (Kibret et al., 2018). Train duration refers to the length of

time the entire series is delivered (i.e., to complete one cycle which includes both positive and negative current flow). Stimulus duration is measured in seconds and can range from 0.5-4 seconds (Devanand et al., 1998). Amplitude is the current strength during the pulse, measured in amperes (A) or milliamperes (mA), and is usually fixed at the ECT device maximum (i.e., 800 mA or 900 mA) (Peterchev et al., 2010).

Titration and dosing

The total number of pulses is a key parameter for seizure induction—every ECT pulse results in depolarization of a large number of neurons and when a sufficient number of pulses is delivered, the cumulative effect at the neuronal level yields a seizure. Peterchev et al. (2010) describes how titration and dosing is done in humans: Contemporary ECT devices regulate the dose by adjusting the number of pulses. This is done through varying the stimulus duration and/or frequency. The number of pulses is equal to the product of the train duration and frequency.

(number of pulses) = (train duration) × 2 × (pulse-pair frequency) = (train duration) × (pulse frequency)

The summary metric used to described ECT dose in modern devices is the tota charge. Totally charge is equal to the product of the current amplitude, pulse width, frequency, and stimulus duration.

(charge) = (current amplitude) × (PW) × 2 × (pulse-pair frequency) × (train duration)

Electrode placement

ECT electrode placement is a major determinant of the spatial distribution of induced electric field and relative degree of stimulation of different brain regions (Peterchev et al., 2010). Different electrode configurations include: bitemporal, bifrontal, and right unilateral (RUL). In

modern ECT application, bifrontal and right unilateral are most commonly used since it leads to less cognitive impairment compared to bitemporal placement (Bailine et al., 2000; Delva et al., 2000).

Anesthesia and muscle relaxants

Historically, ECT was administered without anesthesia, subsequently it was deemed necessary to apply anesthetic and muscle relaxant during stimulation. Doing so reduces side effects from convulsions such as bone fractures, dental and tongue injury, as well as damage to muscles and tendons (Kerner and Prudic, 2014; Leiknes et al., 2012). Modified ECT—with the application of anesthetic and muscle relaxant—has been the recommended protocol in the last decade according to internationally established guidelines (American Psychiatric Association 2001; Royal College of Psychiatrists 2005; Enns et al. 2010; Leiknes et al., 2012). The standard anesthetic agent used in ECT is Methohexital and the most common muscle relaxant used is succinylcholine (Kerner and Prudic, 2014).

1.1.4. Electroconvulsive stimulation (ECS): How ECS is applied in mice

ECS stimulus parameters

The stimulus parameters used in this study are: 20-25 mA, 50 Hz, 0.5 ms pulse width current with 0.5 second duration. These parameters were chosen based on the ability to induce tonic-clonic seizures in GCaMP6 mice based on preliminary experiments. Additionally, the current amplitude in this study is close to the 15.3 mA that simulates a median electric field of 800 mA in human ECT (Bernabei et al., 2014); as it is slightly higher, it likely more closely simulates median electric field of 900 mA, the other common amplitude used in clinical ECT.

Stimulus titration in animal models

Compared to human application that titrates ECT by varying pulse duration and/or frequency, ECS animals models typically titrate the stimulus by varying pulse amplitude. Titration by regulating pulse amplitude was the strategy used in this study—applying 20-25 mA of current. 50 Hz, 0.5 ms pulse width current with 0.5 second duration. These parameters were chosen based on the ability to induce tonic-clonic seizures in GCaMP6 mice and previous studies that used similar parameters. In addition, since pulse amplitude controls the volume of neural tissue directly activated by the induced electric field and amplitude titration could reduce adverse effects during seizure threshold titration procedure. A stepwise rise in pulse amplitude leads to a gradual increase in volume of neural tissue that is activated until a seizure is elicited (Peterchev et al., 2010); hence, avoiding excessive stimulation of larger portions of the brain than is necessary to induce a seizure.

Electrode placement (auricular, corneal, implanted frontal lobe electrodes)

Electroconvulsive stimulation (ECS) is an animal model of ECT. There are three electrode placements used for ECS: earclip, corneal, and more recently, screw electrodes above the motor cortex (Theilmann et al., 2014). Each of these electrode configurations have their own advantages and disadvantages.

It is important to note how electrode placement in animal models compare to human ECT since electrode placement is a crucial determinant of the spread of induced electric field and the relative degree of stimulation of different brain regions (Peterchev et al., 2010). Ear clip electrode is the most commonly used placement (van Buel et al., 2017, Bernabei et al., 2014,

O'Donovan et al., 2014, Weber et al., 2013)—due to its relative ease of application and the requirement of only one experimenter to apply stimulations (versus two for corneal electrodes). A computational model (i.e., a high-resolution finite element mouse model) reveals that to simulate the median electric field of 800 mA in human ECT, the electrode current in the mouse should be set at ~15 mA (Bernabei et al., 2014). Since in human ECT current amplitude is fixed at the device maximum of either 800 or 900 mA (Lee et al., 2016, Deng et al., 2011), the 15.3 mA estimate in median current is close to the 18-25 mA current strength used in previous mouse ECS studies (Bernabei et al., 2014, Chung et al., 2013, Sakaida et al., 2013). However, that computational model shows that the strongest electric field induced by ear clip electrodes is towards posterior brain regions (i.e., cerebellum and midbrain) (Bernabei et al., 2014), while corneal and cortical electrode placement induces the strongest electric field in frontal brain regions. The differences in spatial distribution of current—strongest in posterior or anterior brain regions for auricular electrodes or corneal and frontal electrodes, respectively, present a major disadvantage for the former and a major advantage for the latter.

On the other hand, corneal and cortical electrode placements also present inherent risks. Repeated application of electrodes to the eyes presents the potential for causing injury to the cornea and surgically implanting cortical electrodes carries the risk of accidentally damaging the cortex. Theilmann et al. (2014) implanted screw electrodes in rats. Doing something similar would be less practicable for this study wherein mice are used—the skull and dura mater are substantially thinner in mice compared to rats (Yoder, 2002). This would pose a greater risk of accidental cortical damage in mice.

Despite differences in localization of the strongest electric field between auricular versus corneal or cortical electrode placement, it has been previously shown that they result in similar

behavioural and molecular changes. First, both corneal and auricular ECS induce behavioural seizures of similar duration (Ferraro et al., 1990). Second, cortical (Theilmann et al., 2014), corneal (Lloyd and Sattin, 2015), and auricular (Chang et al., 2017) ECS induce antidepressant-like effect on animal models of depression. Lloyd and Sattin (2015) demonstrates that both auricular and corneal electrode stimulations have equal antidepressant-like properties based on the forced swim test—a widely used measure of antidepressant efficacy (Chang et al., 2017). Third, both corneal and auricular ECS lead to an increase in GABA levels across many brain regions, though with a few regional differences. Auricular ECS increased GABA levels in the following examined regions: frontal cortex, hypothalamus, olfactory bulbs, substantia nigra, and striatum; while no significant change was seen in the hippocampus and nucleus accumbens. Corneal ECS led to increased GABA levels in the hippocampus, frontal cortex, hypothalamus, and olfactory bulbs; a significant decrease in the nucleus accumbens; and no change in the substantia nigra and striatum (Ferraro et al., 1990). At first glance, this may indicate that different electrode placements alters the pattern of regional changes in GABA levels induced by ECS. Alternatively, it is possible that this may be a function of differences in current intensity as rats undergoing corneal ECS needed ~4 times higher current to induce behavioural seizures compared to rats receiving auricular ECS (Ferraro et al., 1990). However, this seems unlikely to be the case since maximal ECS seizure patterns are observed after current application at lower intensities—only 20% above minimal seizure threshold (~25 mA). Moreover, once seizure is initiated the discharge is independent of the stimulus (Ferraro et al., 1990). These changes in GABAergic alterations may play a role in the therapeutic mechanism and/ or unwanted consequences of ECT (i.e., transient memory loss). Previous studies report deficiencies in GABA levels in the cerebrospinal fluid (Gerner and Hare, 1981) and plasma (Petty and Sherman, 1984)

of patients with major depression and also in animal models of depression (Lushcher et al., 2011).

Taken together, the auricular electrode placement is used for this study due to: 1) its relative ease of use; 2) the ability for one experimenter to apply stimulations; 3) its non-invasive nature; 4) behavioural (i.e., antidepressant-like effect, seizure duration) and 5) molecular changes (i.e., region-specific increase in GABA levels) that are similar to corneal and/or cortical electrode placement.

Anesthesia and muscle relaxant

In this study, ECS was done on awake animals without anesthesia and muscle relaxant. There were no signs of injury or lasting discomfort after the stimulation—animals were active, grooming, socializing, and feeding. Anesthetics can cause drug-dependent and dose-dependent neurophysiological changes (Paasonen et al., 2018; Ciobanu et al., 2012). Importantly, several recent studies demonstrate differences in functional network properties between awake and anesthetized animals (Barttfeld et al., 2015, Hamilton et al., 2017, Jonckers et al., 2014, Liang et al., 2015, Ma et al., 2017). Recent work by Paasonen et al. (2018) reports the most comprehensive dataset of how six commonly used anesthesia protocols affect resting state fMRI (rsfMRI) functional connectivity and they show that all six anesthetics studied significantly suppressed functional connectivity of either the thalamus or hypothalamus of rats. This suggests modulation of thalamo-cortical activity by anesthetics. Moreover, they demonstrated that some anesthetics significantly suppressed BOLD spectral power.

Thus, we avoided the confounding effects of anesthetics on functional connectivity and signal spectral power by applying ECS and imaging cortical calcium activity in awake animals.

We evaluated the effectiveness of seizure induction using the Racine scale. Hence, we chose to forgo using muscle relaxants to permit visual observations and ratings of motor seizure behaviour.

1.2. Biophysical mechanisms of ECT

This section briefly discusses the biophysics of ECT, including neural response to the induced electric field and mechanisms of seizure induction. The ECT device applies an electrical current across the electrodes and this induces an electric field. Electrode configuration and head anatomy (i.e., conductivity of the various tissues in the head) determines the electric field distribution in the brain—that is, the strength of electric field in one region of the brain versus another (Peterchev et al, 2010). The strength of the electric field and the volume (Deng et al., 2009) of activated neural tissue can be modulated by adjusting the current amplitude. Hence, the ECT operator can control the electric field characteristics by manipulating the electrode configuration and the stimulus parameters. For a discussion on empirical evidence on the role of individual stimulus parameters (i.e., pulse amplitude, shape, width, frequency, number of pulses), the reader is referred to Peterchev et al. (2010).

1.2.1. Electric current waveform and neural response to induced electric field

In addition to electrode configuration, neural response to ECT is modulated by characteristics of the electric current waveform applied through the electrodes. The ECS unit used in this study, similar to modern ECT devices, produces trains of rectangular constant-current pulses with alternating polarity. The waveform is characterized by amplitude (the current

strength during the pulse), pulse width (PW, the duration of each pulse), pulse-pair repetition frequency (the number of pairs of a positive and a negative pulse per second), and stimulus train duration. The stimulus parameters used in this study are: 20-25 mA, 50 Hz, 0.5 ms pulse width current with 0.5 second duration. These parameters were chosen based on the ability to induce tonic-clonic seizures in GCaMP6 mice based on preliminary experiments. Additionally, the current amplitude in this study is close to the 15.3 mA that simulates a median electric field of 800 mA in human ECT (Bernabei et al., 2014); as it is slightly higher, it likely more closely simulates median electric field of 900 mA, the other common amplitude used in clinical ECT.

The induced electric field causes depolarization and hyperpolarization of neuronal membranes (Peterchev et al., 2010). Which response ensues (depolarization versus hyperpolarization) depends on the polarity of the given stimulus—as the ECT device produces current pulses of alternating polarity, the response is alternating between the two electrodes. Right after the first stimulus pulse, the brain region near the electrode which first delivers anodal pulse hyperpolarizes while the brain region near the opposite electrode, which delivers cathodal pulse first, depolarizes (Bai et al., 2012). Action potentials are initiated beneath the electrode that delivers cathodal pulse, with an overshoot of over 40 mV. The volume of activated brain region transiently expands until it reaches a maximum spatial extent of 1.3- 1.5 cm below the cortical surface. As the activated region reaches late repolarization phase, the activated region ceases to expand. Then, as the second pulse is generated (anodal), the previously activated region begins to hyperpolarize while the contralateral side (receiving cathodal stimulation in the second pulse) begins to depolarize (Bai et al., 2012).

Aside from the polarity of the electrical pulse, current amplitude and pulse width also modulate neural response to the induced electric field. Decreasing the current amplitude by

almost half (i.e., 500 mA instead of the usual 800 mA) decreases the surface area of the excited region as well as the depth of penetration from 1.5 cm to <1 cm from the cortical surface. Additionally, it increases the time for depolarization to reach threshold. In a similar manner, Decreasing pulse width (from the default 1 msec to 0.6 msec) also decreases the volume of excited region, decreases the depth of penetration, while increasing depolarization to threshold time (Bai et al., 2012).

1.2.2. Mechanisms of seizure initiation and propagation

ECT induces generalized seizures in controlled conditions and one important question is whether generalized seizures involve simultaneous activation of separate focal areas or seizure activity begins in one region then propagates to others. Imaging using single photon emission computed tomography (SPECT) during ECT—which reveals cerebral blood flow (CBF) at the time of tracer injection— Enev et al. (2007) demonstrate that 0 s after ECT stimulus is applied, there is increased CBF near the regions of the bitemporal stimulation electrodes, putamen, and thalamus. Interestingly, the late ictal group, wherein the tracer is injected 30 s after ECT stimulus application, shows increased CBF in bilateral parietal and occipital cortices with decreased CBF in the bilateral cingulate gyrus and left dorsolateral prefrontal cortex. The findings support the hypothesis that generalized seizures involve activation of specific brain regions with subsequent propagation of activation to other regions.

What mechanisms are involved in seizure initiation and propagation?

Seizure initiation involves two concurrent events: 1) high-frequency bursts of action potentials, and 2) hypersynchronization of action potentials of a neuronal population. At the single neuron

level, epileptiform activity is characterized by sustained neuronal depolarization that lead to a burst of action potentials. The bursting activity resulting from prolonged depolarization is mediated by the influx of extracellular Ca2+, subsequently opening voltage-gated Na+ channels, leading to influx of Na+, generation repetitive action potentials (Bromfield et al., 2006). The hyperpolarizing afterpotential that follows is mediated by GABA receptors and Cl- influx or K+ efflux, depending on cell type (Bromfield et al., 2006).

When there is sufficient activation to recruit surrounding neurons, seizure propagation—the process by which a seizure spreads across brain regions—occurs. This propagation of burst activity is normally subdued by intact hyperpolarization and surround inhibition by inhibitory interneurons; however, with sufficient activation surrounding neurons are recruited through: 1) increased extracellular K+, which dampens the extent of hyperpolarizing outward K+ currents, tending to depolarize neighboring neurons; 2) accumulation of Ca++ in presynaptic terminals, leading to enhanced neurotransmitter release; and 3) depolarization-induced activation of NMDA receptors, which causes more Ca++ influx and neuronal activation (Bromfield et al., 2006).

1.3. Hypotheses and objectives

Recent work in our lab demonstrates a wide-scale increase in functional connectivity in a mouse model of depression (McGirr et al., 2017). As such, our central hypothesis is that ECT acts to correct aberrant hyperconnectivity observed in neuropsychiatric disorders such as major depression. The overall goal of this project is to examine how neuronal networks change after ECT—emphasizing effects on brain regions that are also relevant to ECT-induced memory loss since impairment of episodic memory is the most prominent side effect of ECT.

Research hypotheses

1) ECS modulates the frequency of neural oscillatory activity in a region-specific manner, and will have the greatest impact on memory-related regions
2) ECS decreases functional connectivity in a depression-related network (i.e., default mode network)

Research objectives

1) To examine how ECS modulates the frequency of neural oscillatory activity in multiple cortical regions
2) To investigate how ECS modulates functional connectivity, particularly in a depression-related network (i.e., default mode network)

Chapter 2: METHODS

2.1. Animals

Transgenic GCaMP6 mice (n = 12, 6 males, 6 females) were used for longitudinal imaging experiments. These were generated by crossing Emx1-cre (B6.129S2-Emx1tm1(cre)Krj/J, Jax #005628), CaMK2-tTA (B6.Cg-Tg(Camk2a-tTA)1Mmay/DboJ, Jax #007004), and TITL-GCaMP6s (Ai94; B6.Cg-Igs7tm94.1(tetO-GCaMP6s)Hze/J, Jax #024104) strains (Madisen et al., 2015). This crossing is expected to produce stable expression of GCaMP6s (Tian et al., 2009; Chen et al., 2013) within all excitatory neurons across all cortical layers (Vanni and Murphy, 2014). Each animal was genotyped through PCR amplification before use in experiments to assess presence of GCaMP expression.

The housing facility had a 12:12 light-dark cycle, with lights on at 07:00 h. Prior to and during imaging and stimulation experiments, mice were housed in groups of two-four. All mice had *ad libidum* access to water and standard laboratory mouse diet. Animal protocols were approved by the University of British Columbia Animal Care Committee and were in accordance with the Canadian Council for Animal Care guidelines.

2.2. Chronic window surgery

Animals were anesthetized with isoflurane (2% in pure O_2) and a through-bone transcranial window was installed as previously described (Vanni et al., 2017, Silasi et al., 2016). Briefly, after locally anesthetizing the scalp with lidocaine (0.1 ml, 0.2%), the skin covering the skull was removed and a glass coverslip was applied using Metabond clear dental cement (Parkell, Edgewood, NY, USA; Product: C&B Metabond). A steel bar was attached such that there was a 4-mm posterior space between the bar edge and bregma—this is for future head-fixation during recordings. This window permits recording of wide-field fluorescence in a

regions covering up to 10x10 mm field of view. Moreover, this imaging window allows longitudinal, repeated imaging sessions from mice extending several months.

2.3. Experimental design

After chronic window surgery, we generally wait 7 days before head-fixed imaging to provide time for the incision to heal. Within this time, mice are handled and habituated to the earclip electrodes used for electroconvulsive stimulation. After removing the electrodes, mice are then gently coaxed into the plexiglass tube to habituate them to the head-fixing apparatus and imaging chamber. After 5 days of habituation, baseline imaging is done for 5 days. Then, ECS was done once per day, every other day, for a total of 10 sessions. This simulates clinical ECT timelines. Imaging was done every single day, both during on and off ECS days, until the end of 10 ECS sessions—for a total of 25 recordings. Imaging sessions last for 20 minutes each time.

2.4. Electroconvulsive stimulation (ECS)

Electrical pulses used to induce ECS were generated by a rodent electroconvulsive device (ECT Unit model 57800; Ugo Basile) and delivered through padded earclip electrodes soaked in saline. The stimulus parameters are as follows: 1 s stimulus duration, 0.5 ms pulse width, 50 Hz frequency, current amplitude at 20-25 mA. Preliminary experiments showed that these parameters induce tonic-clonic seizures lasting approximately 20 s in GCaMP6 mice. Sham animals were handled identical to ECS animals, including attachment of saline-soaked earclip electrodes, without passing electrical current.

2.5. Head-fixation apparatus and imaging chamber

The head-fixation apparatus was designed to provide reproducible fixation of mice with head bars onto steel mounts with indentations. Adjacent to the head-fixing mount, a clear Plexiglass tube (28 mm diameter) was attached to an aluminum baseplate which provides a snug chamber for the mouse to rest during imaging sessions. Following 5 sessions of handling and habituation to the Plexiglas tube, mice can be gently coaxed into the fixation tube. Once the head bar is positioned into the indentation of the head-fixing mount, a sliding panel is tightened on top of the steel mount to secure the head bar using a bolt at the end opposite the indentation. This eliminates movement of the head during recordings. Behavioural imaging of mice under infrared illumination shows that mice do not exhibit much active behaviour during imaging sessions, once habituated. During recordings, mice were placed in an enclosed sensory-isolated imaging recording chamber that was kept dark and insulated with acoustic foam to further reduce ambient sounds.

2.6. Spontaneous wide-field calcium imaging in awake mice

Wide-field imaging was performed using a multi-wavelength strategy in order to correct for epifluorescence signals associated with non-calcium dependent events, as previously described (Xiao et al., 2017). Previous work (Ma et al., 2016; Wekselblatt et al., 2016, Sirotin, 2010) inspired this strategy. Hemodynamic correction is done to offset potential cross-talk effects between fluorescence signal and dynamic changes in absorption of light. Neural activity is accompanied with functional increase in blood volume or oxygenation through the process of neurovascular coupling (Hillman, 2014) and hemodynamic changes have been shown to attenuate detected fluorescence and contaminate fluorescence recordings (Ma et al., 2016). A large contributor to changes in the signal from diffusely reflected light—pertaining to light that

enters the brain, scatters within the cortex, and emerges from the same surface to reach the camera—is hemoglobin absorption (Malonek and Grinvald, 1996).

Our strategy employs a short blue wavelength reference light that is near an isosbestic point of hemoglobin absorption—meaning oxygenated and deoxygenated hemoglobin has the same absorption values—thus, making the signal independent of oxygenation and essentially representing changes in local blood volume. We utilized a Raspberry Picam RGB sensor (Waveshare Electronics RPi Camera F) to independently resolve signals attributed to blood volume changes as blue reflected light, while simultaneously collecting green epi fluorescence (GCaMP6). A 10 mm diameter Chroma 69013m multi-band filter was mounted over the image sensor allowing blue, green, and red signals to be simultaneously obtained in separate channels of the camera RGB sensor with less than 10% cross talk between channels. We used Luxeon LEDs: (1) Royal-Blue (447.5 nm) LUXEON Rebel ES LED with added Brightline Semrock 438/24 nm filter to provide a short blue wavelength reflected light signal that is expected to report blood volume changes; (2) a blue 473 nm Luxeon Rebel ES LED for excitation of GCaMP6 with a Chroma 480 nm/30 nm excitation filter. Preliminary analysis done by Xiao et al. (2017), demonstrates that the short blue signal correlated with apparent blood volume artifacts that were done in experiments that recorded green reflectance signal in parallel with blue reflectance. Imaging was done for 20 minutes. 24-bit RAW RGB image sequences were collected at 30 Hz temporal resolution, 33.3 ms exposure, and auto-white balance turned off.

2.7. Image processing

Data Preprocessing

Data were imported and analyzed using MATLAB (Mathworks, Inc. Natick, MA). Multiple recordings of each mouse across days (i.e., baseline, ON-stimulation, and OFF-stimulation days) were registered by calculating the spatial shift (X, Y) and rotation relative to the first recording using autocorrelation (Murphy et al., 2016, Vanni et al., 2017). For subsequent analyses (i.e., correlation, partial directed coherence, power calculation, etc.), results for time points of interest ((i.e., baseline, ON-stimulation, and OFF-stimulation days) were averaged across days per mouse before being averaged between mice (i.e., ECS versus Sham) for group comparison.

GCaMP fluorescence and short blue reflectance signals were expressed as fractional change relative to baseline ($\Delta F/F_0$) to account for slight differences across pixels in expression, illumination, and detection (Wekselblatt et al., 2016) due to the curvature of the brain at midline and along lateral edges (Silasi et al., 2016). This entails averaging across all frames for each recording to establish a baseline, then the change in fluorescence or reflectance signals from this averaged baseline was calculated for each frame.

The short blue reflectance image stacks were used to normalize fluorescence image to account for changes in absorbance due to hemodynamic coupling. This is important since the excitation and emission bands of GCaMP overlap with varying absorption bands of oxygenated and deoxygenated Hb and decrease the detected fluorescence signals (Ma et al., 2016). Hemodynamic correction was done by subtracting the fraction fluorescence of short blue reflectance from GCaMP fluorescence as previously described by Wekselblatt et al. (2016).

2.8. Spectral analysis

To explore the spectral features of calcium signals, the Fourier transform was processed on the fluorescence images (Vanni et al., 2017, Vanni et al., 2010a,b). This imparts the ability to examine the relative contributions of various frequencies to the overall (calcium) signal (Wallisch et al., 2009). The regional spectral changes associated with a specific frequency band was measured by averaging the power amplitude of Fourier on each pixel of the regions of interest. The frequency bands of interest include: delta (1-4 Hz), theta (4-7 Hz), and alpha (8-12 Hz). These analyses were performed on the full 20 min recordings.

2.9. Network analysis

To infer functional connectivity, 12x12 connectivity matrices were generated from Pearson correlation coefficients of spontaneous GCaMP $\Delta F/F_0$ activity from 12 ROIS (6 ROIs per hemisphere) using custom MATLAB scripts. Pearson r values are based on temporal profiles between one pixel—selected as a seed per ROI—and all other ROI seeds (Mohajerani et al., 2013; Vanni and Murphy, 2014). The following ROIs were characterized: primary motor area (M1), barrel cortex (BC), forelimb somatosensory area (FL), hindlimb somatosensory area (HL), parietal association area (PT), and retrosplenial area (RS). ROI coordinates were defined according to the Allen Institute Atlas and previous studies (Vanni and Murphy, 2014). Self-correlation among ROIs and symmetrical correlations across the diagonal (i.e., upper triangle of correlation values in connectivity matrices) were not included.

Data from the connectivity matrix was used to generate network diagrams. Scripts from the brain connectivity tool box (http://www.brain-connectivity-toolbox.net; Rubinov and Sporns, 2010) were incorporated into the custom MATLAB scripts to create a network diagram based on

the differences from baseline in each condition. A consistent threshold across groups was applied to create network diagrams with only the strongest GCaMP responses. Node size is proportional to the strength of the connections per node (i.e., sum of weights of links connected to the node) and edge thickness between nodes is proportional to the weight of the connections between nodes. Network diagram edges (i.e., links) were color coded to demonstrate changes in network connections over time: red indicates a decrease in strength, green indicates an increase in strength, and gray represents a marginal change (<10%) in strength.

2.10. Statistical analysis

Within-group repeated measures ANOVA, with Bonferroni's post hoc test, were done to elucidate pre-post region-specific changes in power in delta, theta, and alpha bands for each group (ECS and Sham). All values are reported as mean± standard error of the mean (SEM), with a significance value of $p < 0.05$. Additionally, to compare changes in power per ROI between ECS and Sham, unpaired *t* test was also calculated. Node strength between-group comparisons per ROI were also done using unpaired *t* test. The cumulative probability distribution of correlation parameters derived from matrices for functional connectivity analysis was done using one-sample Kolmogorov–Smirnov test.

Chapter 3: RESULTS

Wide-field chronic windows permit a repeated imaging design using GCaMP mice—recording spontaneous cortical activity at three time points: baseline, acute, and 24h post stimulation. Additionally, imaging using GCaMP6 mice allows longitudinal recordings of intracellular calcium which reflect changes in neuronal spiking activity while imaging at a mesoscale captures dynamics of neuronal populations across brain regions. This enables assessment of changes in regional activity and inter-region connectivity after ECS. Figure 1 illustrates the experimental paradigm including mouse strain (Figure 1A), timeline of experiments (Figure 1B), regions of interest (Figure 1C, 1D), and stimulation and imaging setup (Figure 1E, 1F).

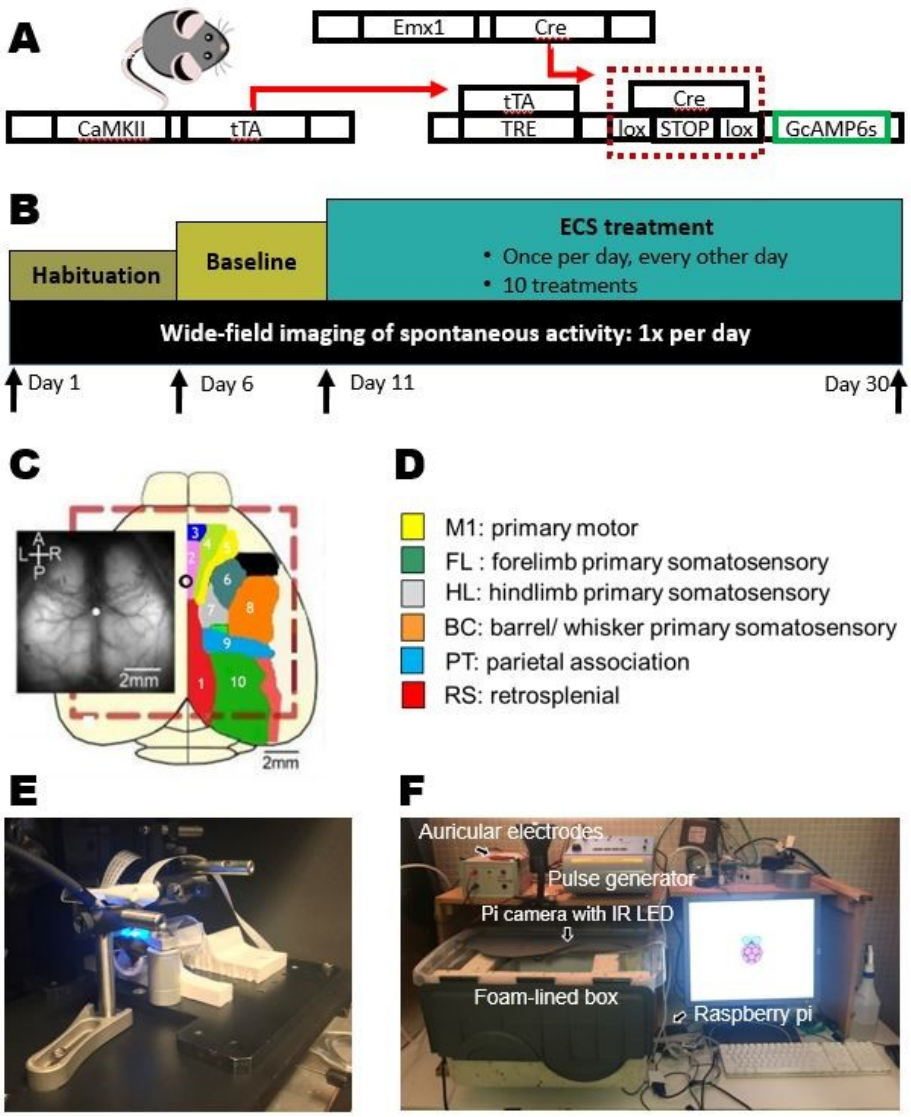

Figure 1 | Experimental design. (**A**) Schematic illustrating the approach used to generate Emx1-cre-CaMKII- GCaMP6s transgenic mice. This crossing is expected to produce stable expression of GCaMP6s (Tian et al., 2009; Chen et al., 2013) within all excitatory neurons across all cortical layers (Vanni and Murphy, 2014). (**B**) Timeline of experiments. First, animals were handled and habituated to the 1) earclip electrodes used for electroconvulsive stimulation (ECS), 2) head-fixing apparatus, and 3) imaging chamber. After 5 days of habituation, baseline imaging is done for 5 days. Then, ECS was done once per day, every other day, for a total of 10 sessions. Imaging was done every single day, both during on and off ECS days. (**C**) Representative view through chronic cranial windows for GCaMP6 imaging. (**D**) Schematic representation of the regions of interest over a single hemisphere. (**E**) Head-fixation apparatus and imaging chamber. (**F**) ECS apparatus and stimulation chamber. Electrical pulses were generated using a rodent ECS device (ECT Unit model 57800; Ugo Basile). Stimulation was done in a foam-lined box. Ictal and post-ictal behaviour was recorded using a Pi camera controlled by Raspberry pi.

3.1. Region-specific changes in power varies across frequency bands after ECS

We sought to determine the effects of ECS on power within the following frequency bands: delta (1-4 Hz), theta (4-7 Hz), and alpha (8-12) Hz. Performing Fourier transform on each pixel individually (Vanni et al., 2010a,b), brain activity associated with each specific frequency band was measured by averaging the power amplitude of Fourier within a frequency window. The Fourier transform decomposes a time series signal (i.e., GCaMP recording) into its constituent frequency components and these frequency components can then be grouped into bands. The absolute value of the decomposed signal represents power—which measures the amount of variance that frequency contributes to the original data. These analyses were implemented on the full 20 min recordings using modified custom MATLAB scripts (Vanni et al., 2017).

3.1.1. Delta (1-4 Hz)

Within-group repeated measures ANOVA reveals region-specific changes in power in the delta band after ECS. There are significant pre-post increases in power in M1, BC, and RS acutely post stimulation, which is maintained 24h after. (Figure 2 A,C) ($*p < 0.05$, $**p < 0.01$, $***p < 0.001$, with Bonferroni's post hoc test). The Sham group did not show any significant difference from baseline in both the acute and 24h period. Additionally, of the ROIs that showed significantly increased power in the delta band after ECS, only RS had a significantly higher power upon comparing to Sham acute effects (unpaired t test: $p= 0.025353644$). This between group difference was undetectable after 24h.

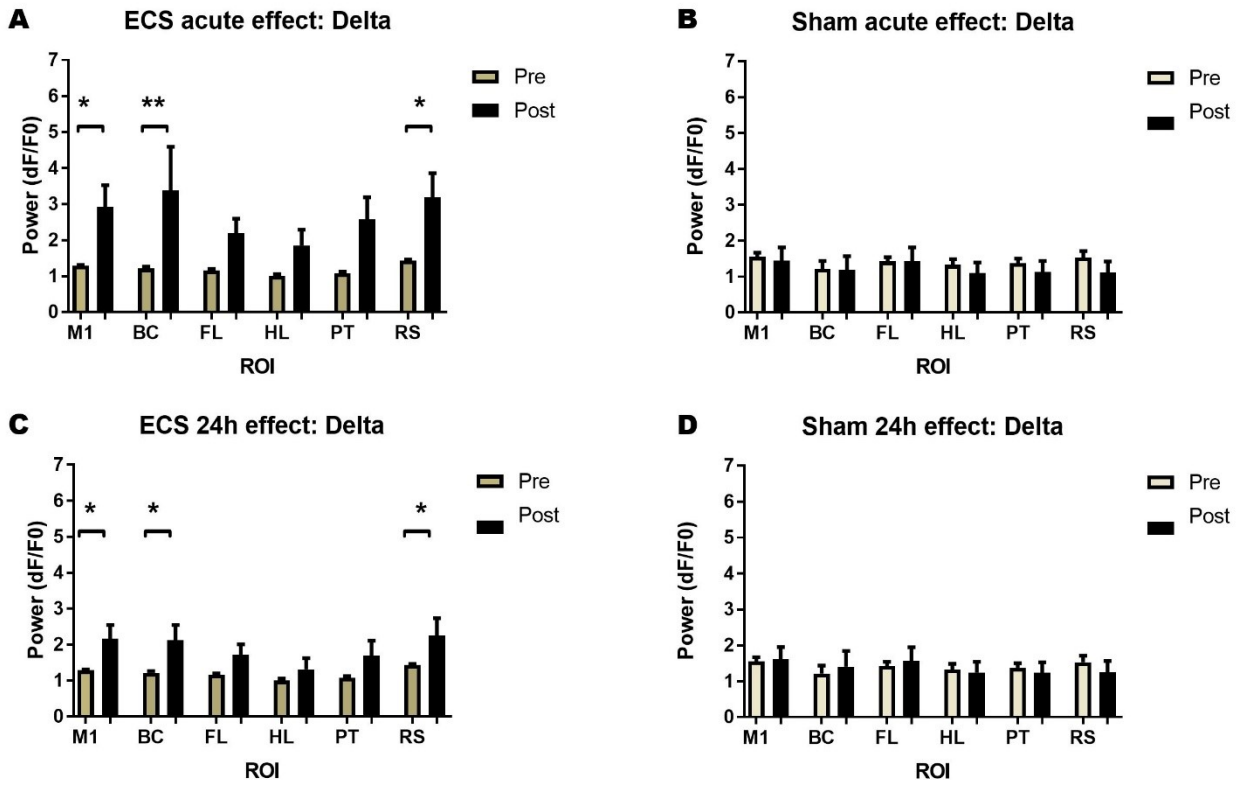

Figure 2 | ECS increases delta power in M1, BC, and RS. (**A**) Delta power per ROI after ECS (acute), ∗p < 0.05, ∗∗p < 0.01, ∗∗∗p < 0.001, within-group repeated measures ANOVA (baseline and acute post ECS or baseline and 24h post ECS) with Bonferroni's post hoc test. (**B and D**) Sham delta power per ROI in the acute and 24h period, respectively. (**C**) Delta power per ROI after ECS (24h), ∗p < 0.05, ∗∗p < 0.01, ∗∗∗p < 0.001, within-group repeated measures ANOVA with Bonferroni's post hoc test, (n = 6, Sham versus n = 6, ECS). Delta is normalized by total power of the Fourier transform. Error bars reflect standard error of the mean (SEM). Results reflect mean power from 10 ECS on (acute) and off (24h) days.

3.1.2. Theta (4-7 Hz)

Within-group repeated measures ANOVA in the theta band reveals increase in power in BC acutely after ECS and this increase persists 24h after (Figure 3 A, C) (∗p < 0.05, ∗∗p < 0.01, ∗∗∗p < 0.001, with Bonferroni's post hoc test). On the other hand, upon comparing between groups, the RS shows a significant increase in power in the acute post-stimulation period (unpaired t test: p= 0.016458805) and PT is approaching significance (unpaired t test: p=

0.06784686). and this between group difference in RS and PT is not statistically significant 24h after (unpaired t test p= 0.084437417, p=0.182647926, respectively).

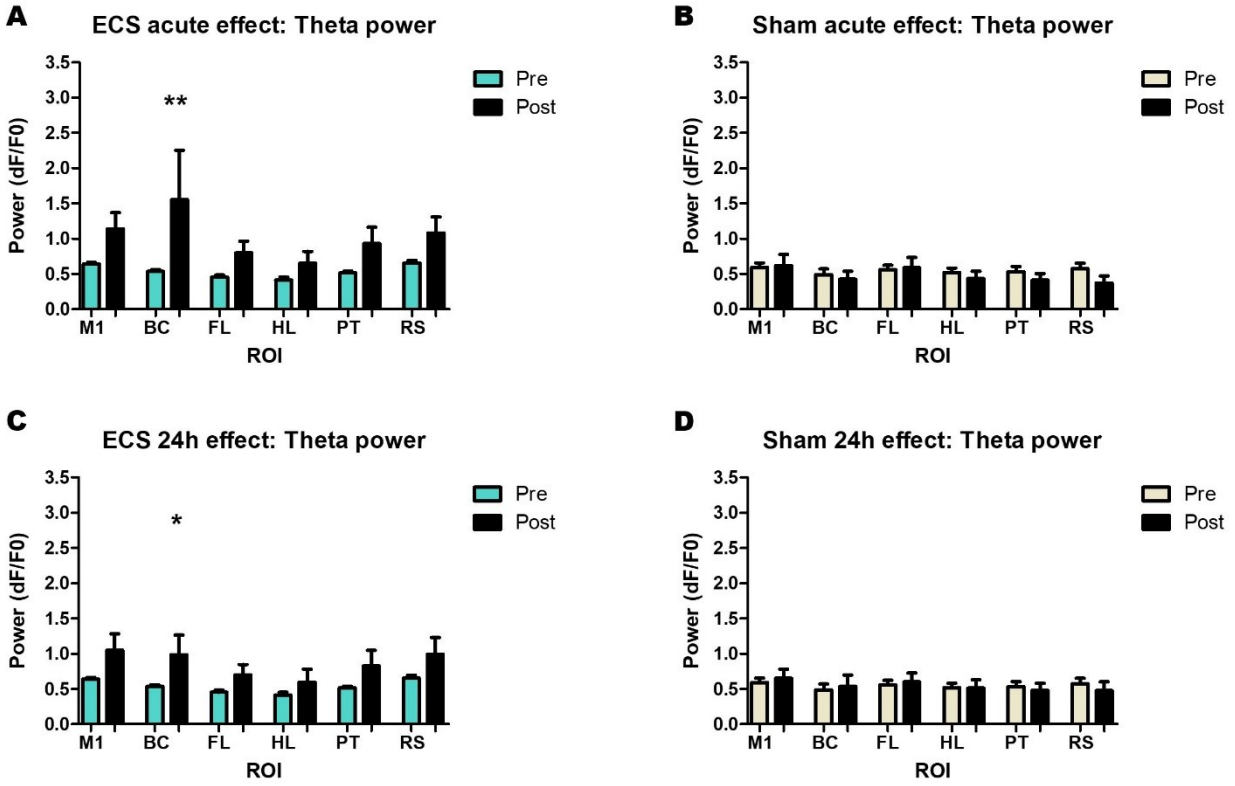

Figure 3 | ECS increases theta power in BC. (**A**) Theta power per ROI after ECS (acute), ∗p < 0.05, ∗∗p < 0.01, ∗∗∗p < 0.001, within-group repeated measures ANOVA (baseline and acute post ECS or baseline and 24h post ECS) with Bonferroni's post hoc test . (**B and D**) Sham Theta power per ROI in the acute and 24h period, respectively. (**C**) Theta power per ROI after ECS (24h), ∗p < 0.05, ∗∗p < 0.01, ∗∗∗p < 0.001, within-group repeated measures ANOVA with Bonferroni's post hoc test, (n = 6, Sham versus n = 6, ECS). Theta is normalized by total power of the Fourier transform. Error bars reflect standard error of the mean (SEM). Results reflect mean power from 10 ECS on (acute) and off (24h) days.

3.1.3. Alpha (8-12 Hz)

Notably, compared to other frequency bands, it is evident that the change in power in the alpha band has an opposite effect—a decrease in power in multiple ROIs in both ECS and Sham animals. Within-group repeated measures ANOVA demonstrates a decrease in power in BC, FL,

HL, and RS acutely after ECS, while showing a decrease in power in across all ROIs in animals acutely after Sham treatment (Figure 4A, B) ($*p < 0.05$, $**p < 0.01$, $***p < 0.001$, with Bonferroni's post hoc test). 24h after, there is a decrease in power across all ROIs in both ECS and Sham mice (Figure 4 C, D) ($*p < 0.05$, $**p < 0.01$, $***p < 0.001$, with Bonferroni's post hoc test). Remarkably, upon comparing between groups per ROI, ECS animals show higher power compared to Sham mice in BC, PT, and RS acutely after ECS (unpaired t test p= 0.044646034, p=0.040995931, p= 0.029128785, respectively). 24h after, only BC approaches statistical significance at p= 0.074666012.

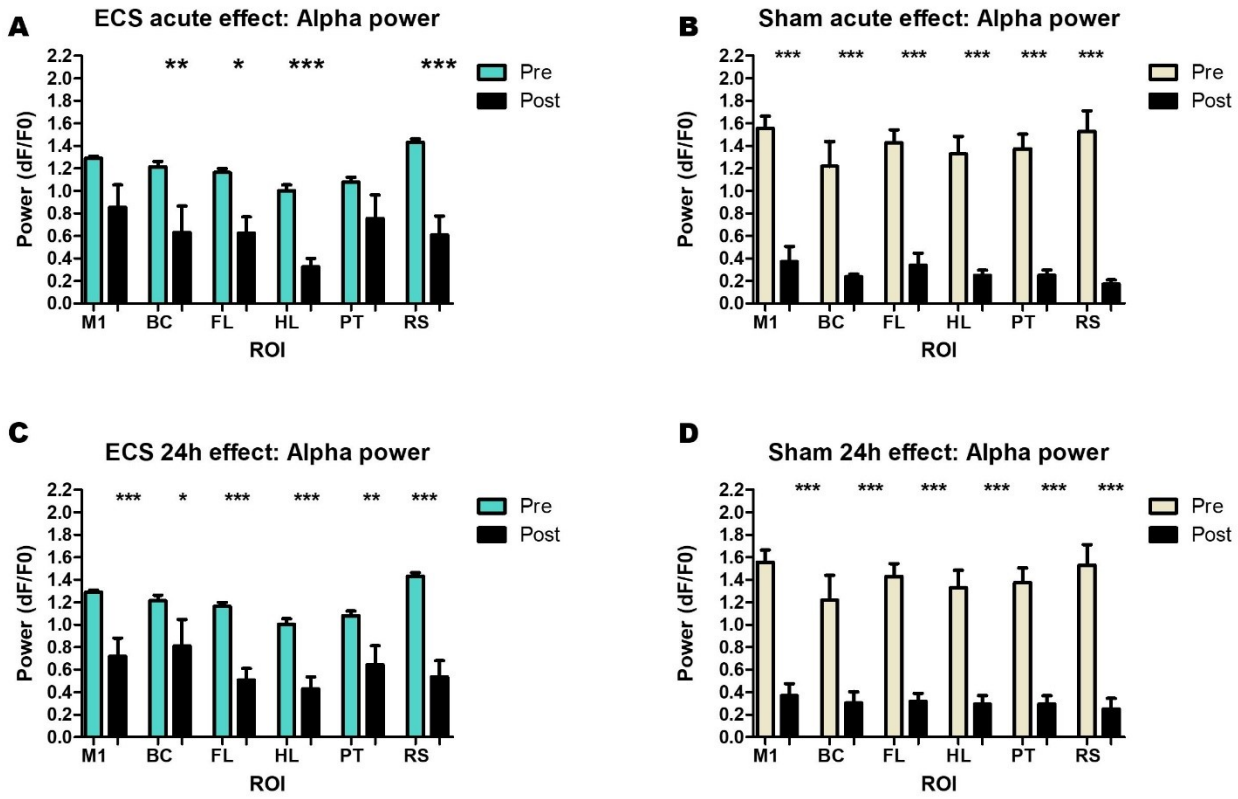

Figure 4 | Wide-scale decrease in alpha power in both ECS and Sham. (**A**) Alpha power per ROI showing a decrease in BC, FL, HL, and RS after ECS (acute). (**B and D**) Sham Alpha power per ROI in the acute and 24h period, respectively, showing decreased power across all ROIs. (**C**) Alpha power per ROI after ECS (24h), showing a wide-scale decrease across all ROIs. $*p < 0.05$, $**p < 0.01$, $***p < 0.001$, within-group repeated measures ANOVA (baseline and acute post ECS or baseline and 24h post ECS) with Bonferroni's post hoc test done on both

ECS and Sham (n = 6, Sham versus n = 6, ECS) for acute and 24 timepoints. Alpha is normalized by total power of the Fourier transform. Error bars reflect standard error of the mean (SEM). Results reflect mean power from 10 ECS on (acute) and off (24h) days.

3.2. Functional connectivity

3.2.1. Acute effects: Increased functional connectivity after ECS

To infer functional connectivity changes, 12x12 connectivity matrices were generated from Pearson correlation coefficients of spontaneous GCaMP $\Delta F/F_0$ activity from 12 ROIS (6 ROIs per hemisphere) using custom MATLAB scripts. Pearson r values are based on temporal profiles between one pixel—selected as a seed per ROI—and all other ROI seeds (Mohajerani et al., 2013; Vanni and Murphy, 2014). Data from the connectivity matrix was used to generate network diagrams. As illustrated in the network diagrams, node size is proportional to the strength of the connections per node (i.e., sum of weights of links connected to the node) and edge thickness between nodes is proportional to the weight of the connections between nodes. Network diagram edges (i.e., links) were color coded to demonstrate changes in network connections over time: red indicates a decrease in strength, green indicates an increase in strength, and gray represents a marginal change (<10%) in strength.

The network diagram illustrates a global increase in functional connection strength between multiple ROIs acutely after ECS. (Figure 5 C, D) This is further illustrated by seed pixel correlation maps showing enlarged territory in ECS mice relative to control mice (Figure 5 A, B). The statistical differences in cumulative distribution of correlation parameters (*r values*) derived from the connectivity matrices for functional connectivity analysis was assessed using the Kolmogorov–Smirnov (KS) test. Initially, the two-sample KS test was done to compare baseline *r* values between Sham and ECS. This revealed that there is a difference in the

distribution of r values between groups at baseline (p = 1.1430e-05). As such, to examine whether electrical stimulation results in a change from baseline values of connectivity parameters, one-sample KS test was done within each group. This demonstrated a significant increase in connection strength compared to baseline in ECS mice (one-sample Kolmogorov–Smirnov test: p = 1.4257e-07) (Figure 5F), whereas Sham animals also show a significant increase in connection strength compared to baseline (Figure 5E), —albeit to a lesser degree compared to ECS (one-sample Kolmogorov–Smirnov test: p = 0.0265). However, visual inspection of the network diagrams illustrates that there is a difference in where the increases in connectivity are for each group—the increase in functional connectivity right after stimulation appears more anteriorly located in ECS mice, while the increase in Sham mice appears to be greater in posterior cortical regions. The quantification of this is described in a subsequent subsection.

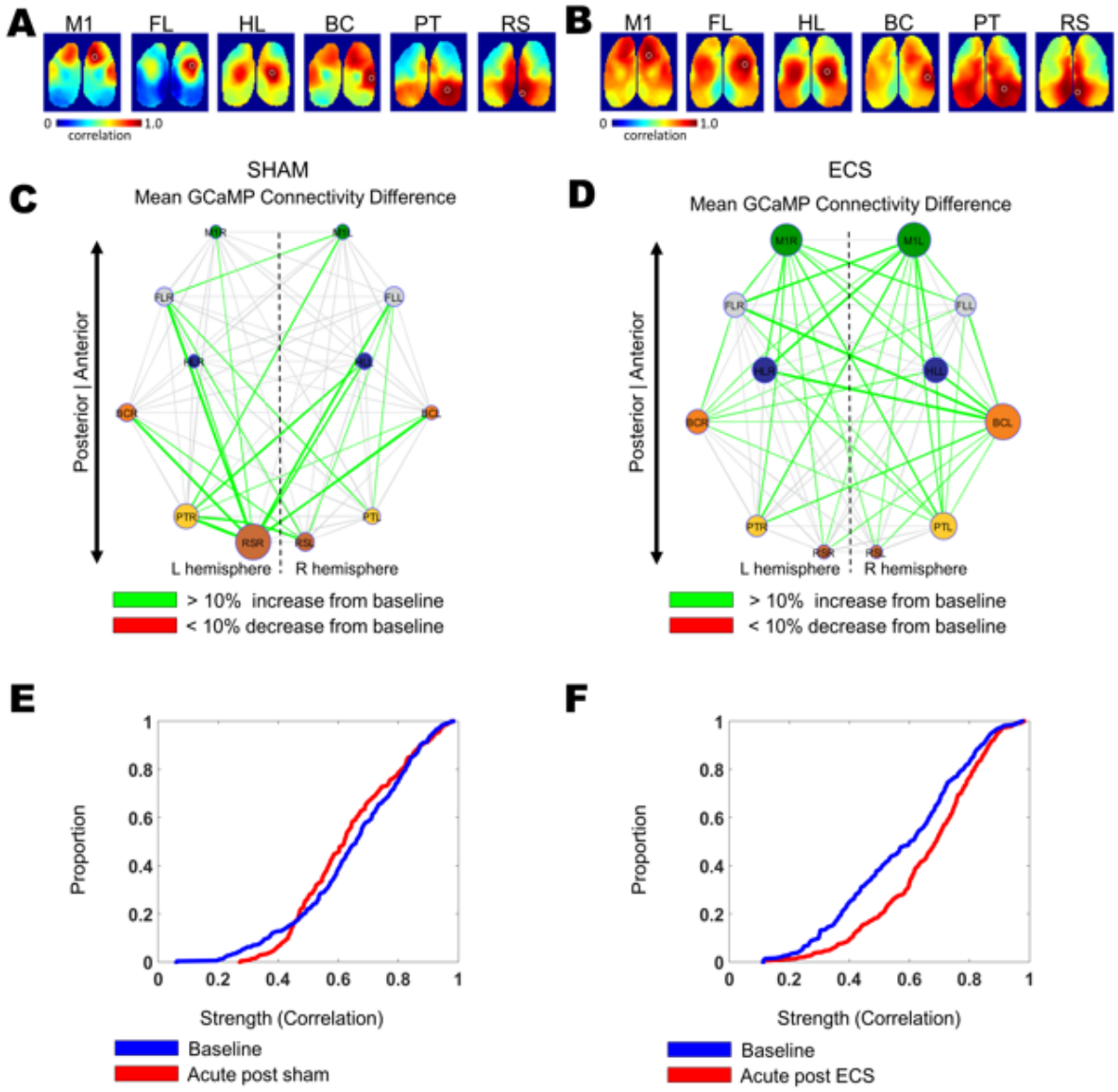

Figure 5 | Acute effect (5-10 min post ECS): Greater increase in functional connectivity in ECS versus Sham. (**A and B**) Seed pixel correlation maps showing an expansion of correlated territories in ECS relative to Sham animals. (**C**) Change in inter-region correlation strength in Sham (acute post - baseline). (**D**) Change in inter-region correlation strength from pre to post ECS (acute post - baseline). (**E**) Sham: cumulative probability distribution analysis of connectivity parameters (*r values*), $p = 0.0265$, one-sample Kolmogorov–Smirnov test. (**F**) ECS: cumulative probability distribution analysis of connectivity parameters (*r values*), $p = 1.4257e\text{-}07$, one-sample Kolmogorov–Smirnov test, (n = 6, Sham versus n = 6, ECS).

3.2.2. 24h effects: Decreased functional connectivity after ECS

Remarkably, the network diagram illustrates a global decrease in functional connection strength between multiple ROIs 24h after ECS—a change in the opposite direction compared to acute effects (Figure 6C, D). Likewise, this is further illustrated by seed pixel correlation maps showing decreased territory in ECS mice relative to control mice (Figure 6A, B). The cumulative distribution of connectivity parameters (*r values*) derived from the connectivity matrices reveals a decrease in connection strength compared to baseline in ECS mice (one-sample Kolmogorov–Smirnov test: $p = 0.0019$) (Figure 6F), whereas Sham animals do not show a statistically significant change in connection strength compared to baseline (Figure E), (one-sample Kolmogorov–Smirnov test: $p = 0.0857$).

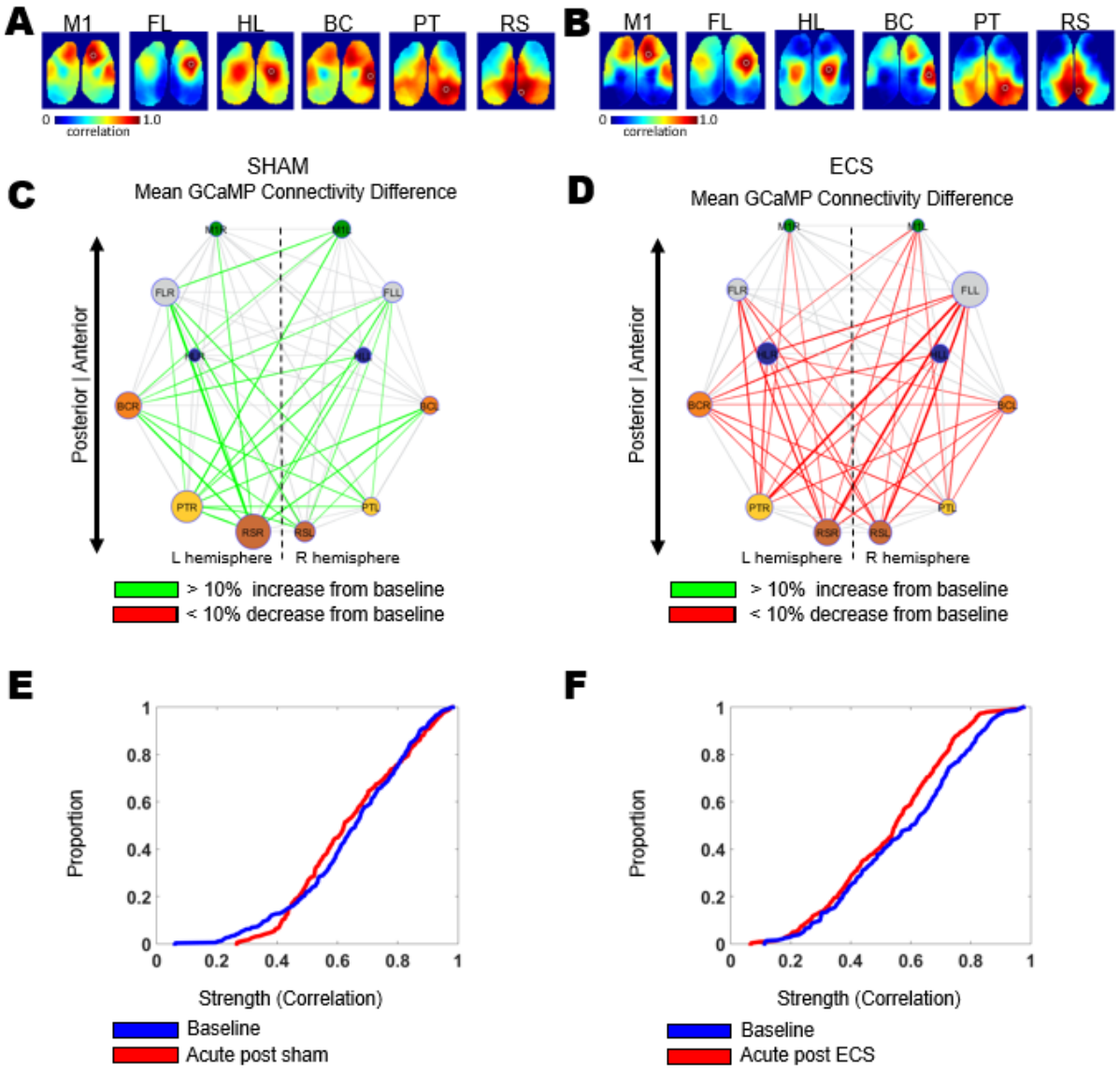

Figure 6 | 24h effect: Decreased functional connectivity in ECS versus Sham. (**A and B**) Seed pixel correlation maps showing a reduction of correlated territories in ECS relative to Sham animals. (**C**) Change in inter-region correlation strength in Sham (24h post - baseline). (**D**) Change in inter-region correlation strength from pre to post ECS (24h post - baseline). (**E**) Sham: cumulative probability distribution analysis of connectivity parameters (*r values*), $p = 0.0857$, one-sample Kolmogorov–Smirnov test. (**F**) ECS: cumulative probability distribution analysis of connectivity parameters (*r values*), $p = 0.0019$ one-sample Kolmogorov–Smirnov test, (n = 6, Sham versus n = 6, ECS).

3.3. Acute and 24h changes in node strength after ECS are region-specific

Upon visual inspection of the connectivity diagrams from Figure 1, it appears that the increase in functional connectivity right after ECS seems to be more anteriorly located, while the slight increase in Sham mice appears to be greater in posterior cortical regions. Remarkably, 24h after ECS, the decrease in connectivity appears to be more uniform across the dorsal cortex, though lesser in M1. On the other hand, in Sham animals it appears to be similar to the acute period. To quantify this, we plotted the node strength per ROI in ECS and Sham animals in both the acute and 24h post stimulation period. This allows us to examine regional differences in strength of connectivity after ECS. Node strength indicates the sum of weights of edges (i.e., links) connected to a node (i.e., brain region). Increase in weight signifies increase in strength of connections between two nodes and increase in node strength reflects increased functional connections between one node and all other nodes connected to it.

Indeed Figure 7 illustrates that there is an anterior trend for the greatest increase in node strength acutely after ECS while this becomes more uniform across ROIs, with the least decrease in M1, 24h after stimulation. When comparing between groups, there is a significant increase in M1 in ECS versus Sham mice (unpaired t test $p= 0.009954688$) and 24h after, there is a significant decrease in RS (unpaired t test $p= 0.03474923$). The change also approaches significance in FL and PT (unpaired t test $p= 0.061147669$, $p= 0.06541369$, respectively). These finding demonstrate that ECS results in an increase in strength of connectivity exhibiting an anteroposterior gradient—with the highest increase in M1. Furthermore, 24h after ECS there is a decrease in strength of connections between ROIs which becomes more uniform, except for M1 which shows the least decrease, and upon comparing between groups this difference is

statistically significant in RS—which is posteriorly located. Thus, ECS effects on functional connectivity is location specific (anterior vs posterior) and time-dependent (acute vs 24h).

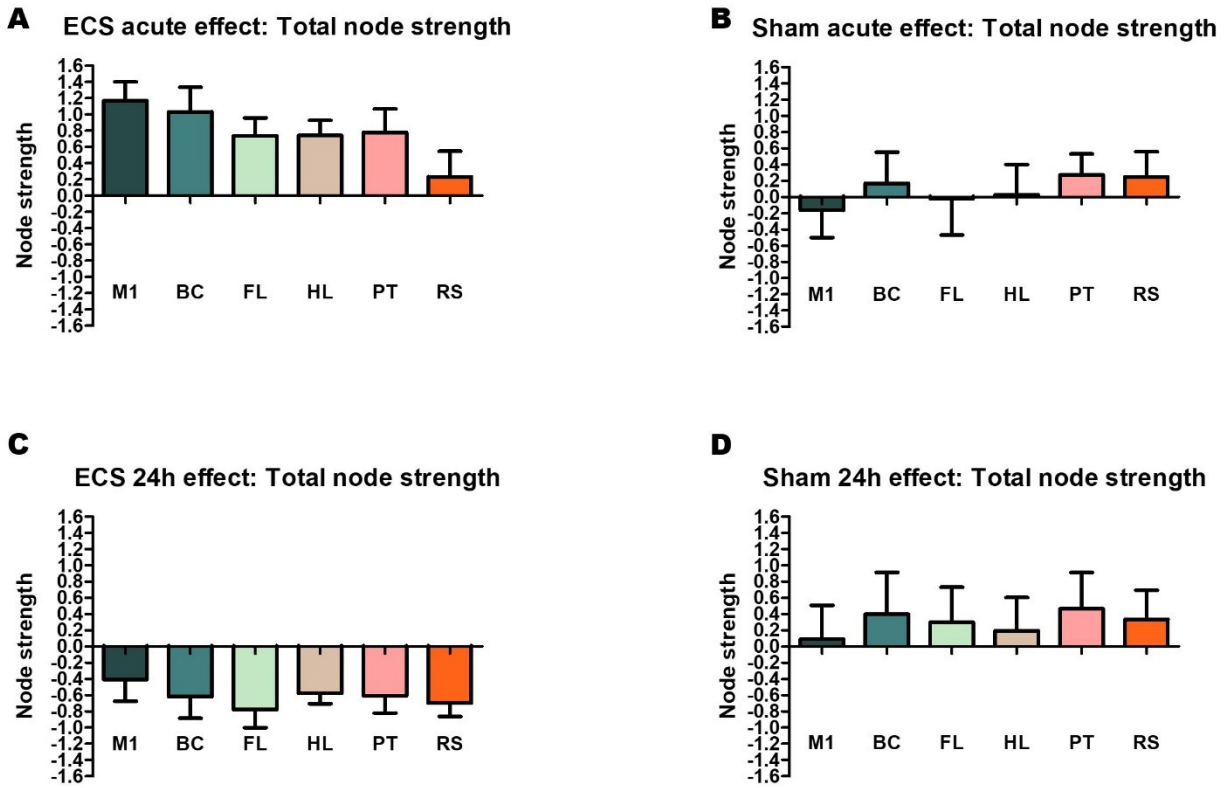

Figure 7 | Acute and 24h changes in node strength after ECS are region-specific. (**A and B**) Change in total node strength from baseline calculated per ROI acutely after stimulation in ECS and Sham animals, respectively, (n = 6, Sham versus n = 6, ECS). Between group comparisons per node shows a significant increase in M1 in ECS versus Sham mice (p= 0.009954688, unpaired t test). (**C and D**) Change in total node strength per ROI 24 post stimulation in ECS and Sham animals, respectively. Between group comparisons per node shows a significant decrease in RS in ECS versus Sham mice (p= 0.03474923, unpaired t test).

Chapter 4: DISCUSSION

4.1. Summary of findings

This study presents the first to achieve longitudinal imaging of neuronal spiking activity at a population-level after ECS—with millisecond temporal resolution spanning a broad expanse of cortex using widefield calcium imaging. The findings in this study recapitulate many large scale functional connectivity alterations observed in humans after ECT using ECS as the analogous animal model. In accordance with effects in humans after ECT (Wang et al., 2018, Cano et al., 2016, Perrin et al., 2012, and Beall et al. 2012), we found a decrease in functional connectivity 24h after ECS. Remarkably, the acute post-stimulation period reveals an increase in functional connectivity. This study is the first to show time-dependent changes in functional connectivity in response to ECT—notably, pioneering the ability to assess functional connectivity changes in the immediate post-ictal period using *in vivo* calcium imaging. The greatest change in node strength (i.e., the sum of weights of links connected to the node) acutely after ECS is highest and statistically significant in M1 when compared to Sham animals. On the other hand, this is statistically significant in RS 24h after ECS versus Sham mice. Thus, ECS effects on functional connectivity is location specific (anterior vs posterior) and time-dependent (acute vs 24h). In addition, the results indicate region-specific changes in power in different frequency bands. There is a strong increase in power in delta (1-4 Hz) in M1, BC, and RS acutely after ECS and these changes are still present 24h after. Similarly, a modest yet significant increase in power is observable in the theta band, and it is more localized in the BC. This increase also persists 24h after ECS. These changes in the delta and theta bands are absent in Sham animals. Moreover, an opposite effect is seen in the alpha band (8-12 Hz) wherein there is a large-scale decrease in power in all ROIs acutely after ECS that is still present in 24h.

Surprisingly, this decrease is also observable in Sham animals. In fact, the decrease in alpha power is more pronounced in Shams particularly in BC, PT, and RS.

4.2. Physiologic significance of power

To better understand the physiologic significance of regional changes in power after ECS, it is important to first elucidate the theory behind spectral analysis based on Fourier transform, particularly as it pertains to calcium imaging data. As an action potential triggers calcium influx via voltage-gated calcium channels, conformational changes in GCaMP lead to an increase in emitted fluorescence. Calcium sensors (i.e., GCaMP6) measure fluctuations in cytosolic free calcium concentration (Grienberger and Konnerth, 2012) and these fluctuations are recorded in the fluorescence images. The oscillation frequency of the calcium transients is calculated by performing the Fourier transform on the fluorescence images. The Fourier transform expresses a signal from the time domain to the frequency domain (Uhlen, 2004) as a sum of sinusoidal components—akin to expressing a musical chord as the frequencies (or pitches) of its constituent notes. In the case of images, these are sinusoidal variations in brightness across the image. From the Fourier transformation of the signal, power is calculated as the square of the amplitude of the wave (Lyons, 2010). The amplitude is a measure of how far, and in what direction (positive or negative), a variable differs from zero (i.e. the average brightness of the whole image) (Lyons, 2010). Since in the case of images we extract the sinusoidal variations in brightness, then amplitude and power (i.e., amplitude squared) reflect how far the signal varies from the average brightness of the whole image. Calcium imaging time series are highly correlated with concurrent local field potential (LFP) recordings (Rosch et al., 2018) which reflect the summed electric current flow from multiple nearby neurons—though

calcium recordings have slower temporal resolution compared to LFP recordings. As such, power—in the case of mesoscale imaging—reflects fluctuations in neuronal population activity associated with a specific frequency or frequency band. Through the Fourier transformation of fluorescence images, we have the ability to examine the relative contributions of various frequencies to the overall (calcium) signal.

4.3. ECS induces region-specific slowing of activity within cortical regions

The combination of changes in power in various frequency bands provides evidence that ECS results in region-specific slowing of cortical activity. There is a strong increase in delta band (1-4 Hz) power in M1, BC, and RS acutely after ECS and these changes are still present 24h after. Similarly, a modest yet significant increase in power is observable in the theta band, and it is more localized in BC. This increase also persists 24h after ECS. These changes in the delta and theta bands are absent in Sham animals. Remarkably, an opposite effect is seen in the alpha band (8-12 Hz) wherein there is a widescale decrease in power across ROIs acutely after ECS that is still present in 24h. Surprisingly, this decrease is also observable in Sham animals. In fact, the decrease in alpha power is more pronounced in Sham particularly in BC, PT, and RS.

The changes in power in delta, theta, and alpha bands recapitulate ECT effects observed in humans and animal models. The slowing of waveforms is the most replicated finding and is associated with positive clinical outcomes (Singh and Kar, 2017). Intracranial recordings in non-human primates (Cycowicz et al., 2008) and EEG recordings in humans demonstrate increased delta band power (Fink, 2002;, Sackheim et al., 1996). Increased delta activity has been linked to clinical efficacy (Fink, 2002;, Sackheim et al., 1996) and the onset of therapeutic response

depends upon the rapidity as well as the extent of slowing of EEG waves (Folkerts, 1996). Moreover, increase in theta power has also been reported after ECT—raised theta activity was shown to be associated with attenuation of psychotic symptoms in patients with psychotic depression (McCormick et al., 2009; Sackheim et al., 1996). Finally, Zhao et al. (2016) revealed that ECT results in decreased alpha activity.

In this study, the regions with the most prominent slowing of neural oscillations are M1, BC, and RS—characterized by increased delta (and theta for BC), as well as decreased alpha. Previous retrograde, anterograde, and optogenetic photostimulation studies reveal anatomical and functional connections between these and related regions. The retrosplenial cortex receives inputs from M1, M2 (secondary motor), and the hippocampus (Yamawaki et al., 2016; Todd and Bucci, 2015; Shibata and Naito, 2008). In turn, RS projects to M2, suggesting a functional link between hippocampal networks involved in spatial memory and navigation and neocortical networks involved in sensorimotor integration and motor control (Yamawaki et a.l, 2016). Moreover, BC projects to both M1 (Mao et al., 2011) and RS (Zakiewicz et al., 2014); Shibata and Naito, 2008). These cortico-cortical connections have also been associated with coupling motor and sensory signals that might mediate sensorimotor integration and motor learning (Mao et al., 2011). Thus, the slowing of oscillations in M1, BC, and RS after ECS provides evidence that ECS modulates sensorimotor integration, motor control, and memory.

Oscillatory activity at various frequency bands have been linked to specific functions. Delta band activity has been associated with learning, motivation and reward processes (Knyazev, 2007 and Steriade et al., 1993), as well as to memory encoding and retrieval (Ekstrom and Watrus, 2013). Theta band activity has been correlated with working memory, emotional arousal and fear conditioning (Knyazev, 2007). Activity in the alpha band has been linked to a

functional mechanism of attention by suppressing the processing of distracting information (Bonnefond and Jensen, 2013) and is thought to mediate top-down inhibitory control and timing of cortical processing (Klimesch et al., 2007).

Recent works suggest that brain regions do not have a single oscillatory rhythm (Mantini et al., 2007); rather, a combination of these rhythms interact to enable a unified cognitive function and coherent behaviour. At the cellular level, detailed biophysical studies illustrate that even single neurons have complex dynamics—demonstrating the capacity to oscillate at multiple frequencies (Mantini et al., 2007, Buzsaki and Draguhn, 2004). Large-scale integration—referring to the series of processes whereby the brain coordinates activity distributed over distant regions—may be generated by dynamic links among brain regions, links that are mediated by synchrony over multiple frequency bands (Varela et al., 2001). Synchrony over different frequency bands have been demonstrated in many contexts, highlighting the interplay between low and high frequencies (Fries et al., 2001; von Stein et al., 2000; Bartos et al., 1999). It is possible that different frequency bands carry complementary dimensions of the integration process (Varela et al., 2001). These findings emphasize the importance of analyzing multiple frequency bands simultaneously, rather than limiting analysis to one or two bands.

The cellular mechanisms and the downstream effect of the slowing of cortical oscillations after ECT are unknown. It is plausible that the slower rhythms may provide the slower temporal framing within which fast beta and gamma rhythms operate (Varela et al., 2001). Beta oscillations have been shown to be robust in establishing long distance synchrony while gamma rhythms may serve to build local patches of synchrony (Kopell et al., 2000; von Stein et al., 1999). How the combination of changes in various frequency bands (increased delta and

theta, decreased alpha) in specific regions interact and the subsequent effects on neurophysiology and behaviour remain undetermined and open for further investigation.

4.4. Functional connectivity based on seed-pixel correlation

The close association between abnormalities in neuronal synchronization and cognitive dysfunctions emphasizes the importance of temporal coordination of neural oscillations (Uhlhaas and Singer, 2006). Thus, in addition to analyzing regional activity by computing power across frequency bands, it is of interest to examine correlated activity between brain regions due to its clinical relevance. Mapping resting-state functional connectivity in mouse cortex can be performed using imaging modalities with temporal resolution spanning from sub-milliseconds, to milliseconds, to seconds (i.e., voltage-sensitive dye imaging, wide-field calcium imaging, fMRI, respectively). The millisecond resolution of wide-field calcium imaging permits assessment of neural synchrony.

To examine functional connectivity, we employed seed-pixel correlation analysis. This involves generating connectivity matrices from the cross-correlation r values between the temporal profiles of one pixel—selected as a seed per ROI—and all other ROI seeds (White et al., 2011; Mohajerani et al., 2013; Vanni and Murphy, 2014). This was done on the full 20 minute calcium recordings. Functional connectivity analysis was within the delta frequency band. In humans, delta activity is observed not only during sleep or reduced alertness (Knyazev et al., 2012, Hlinka et al., 2010), but also when at rest while awake (Alper et al, 2006, Chen et al., 2008). In rodents, delta activity predominates during quiet wakefulness (Mohajerani et al., 2010, 2013). Moreover, in this study, spectral analysis revealed the delta band has the most prominent increase in power after ECS compared to other frequency bands. As such, we

examined how ECS affects resting-state functional connectivity within the delta frequency band. ECT effects on correlated activity between regions in other frequency bands are interesting topics for future work.

4.5. Changes in functional connectivity after ECT are time-dependent

Numerous neuroimaging studies have provided evidence that ECT modifies connectivity within and between functional networks in the brain. These effects may serve to normalize aberrant neural activity within and between networks—attenuating abnormal hyperconnectivity and correcting anomalous hypoconnectivity. The current work provides evidence that the changes in connectivity after ECT are dynamic—starting with an acute post-ictal decrease in connectivity and evolving to an increase in connectivity 24h after stimulation.

In accordance with effects in humans after ECT (Wang et al., 2018, Cano et al., 2016, Perrin et al., 2012, and Beall et al. 2012), we found a decrease in functional connectivity 24h after ECS. Remarkably, the acute post-stimulation period reveals an opposite effect. The widescale increase in connectivity in the acute post-ictal period may reflect seizure termination dynamics (Bauer et al., 2017, Jirsa et al., 2014, Kramer et al., 2012). Indeed, previous work demonstrates that in the approach to seizure termination, brain electrical activity—as measured through EEG, ECoG, and LFP—exhibit the following dynamical signatures: increased temporal correlation, decreased dominant oscillation frequency, and flickering (i.e., when noise pushes a bistable system back and forth between two alternative states) (Kramer et al., 2012, Scheffer et al., 2009). Additionally, Jirsa et al. (2014) show that spikes—referring to afferent signals that produce post-synaptic potentials reflecting population dynamics—continue after the end of the seizure and is characterized by logarithmic scaling of interspike intervals from seizure offset. In

line with previous work, we found a widespread increase in functional connectivity—based on seed pixel correlation—in the acute post-ictal period. We also found evidence for decreased dominant oscillation frequency based on spectral analysis with the delta band (1-4 Hz) showing the most prominent increase in power compared to other frequency bands. Both the increase in temporal correlation and slowing of dominant oscillation frequency recapitulate previous evidence on seizure termination dynamics at the neuronal population level.

Interestingly, 24h after electrical stimulation reveals a shift to a decrease in functional connectivity. This may reflect reduction in cortical excitability as seen in patients 24 h after a generalized tonic-clonic seizure (Badawy et al., 2009)—the type of seizure induced by ECT and ECS. However, investigations examining changes in excitability after ECT have yielded conflicting results. Sommer et al. (2002) and Bajbouj et al., (2005) demonstrate decreases in cortical excitability after a full course of ECT while Chistyakov et al., (2005) and Casarrotto et al., (2013) show an increase in excitability. Technical differences that potentially contribute to this discrepancy include: 1) location where cortical excitability was measured (i.e., hand region of the motor cortex, vertex, or prefrontal cortex), and 2) ECT electrode placement (bilateral versus right unilateral). Indeed, it has been demonstrated that excitation threshold varies with cortical location (Stewart et al. 2001; Boroojerdi et al. 2002; Gerwig et al. 2003). Further, excitability in different regions is reflected in distinct frequency bands (Samaha et al. 2017). With regards to the differences in ECT electrode placement, it is interesting to note that the works of Chistyakov et al., (2005) and Casarrotto et al. (2013) which show an increase in cortical excitability 24h after ECT both use right unilateral electrode placement. On the other hand, Sommer et al. (2002) and Bajbouj et al. (2005) whose works demonstrate a decrease in cortical excitability after ECT both apply right unilateral electrode stimulation. It is important to note the differences in electrode

placement since electrode configuration is a crucial determinant of the spread of induced electric field and the relative degree of stimulation of different brain regions (Peterchev et al., 2010). Moreover, the brainstem has been shown to be activated during right unilateral and not in bifrontal nor bitemporal electrode placements (Bai et al., 2012). It is likely that both variations in electrode placement which subsequently affect the degree of stimulation of various brain regions, as well as the differences in regions where excitability was measured contribute to the discrepancy in changes in cortical excitability measurements after ECT. As to how the activation of deeper brain structures potentially mediate the differences in cortical excitability and connectivity is beyond the scope of this thesis.

4.6. M1 may mediate seizure termination

We then applied further graph theoretical measures (i.e., node strength) to examine regional differences in strength of connectivity after ECS. Node strength indicates the sum of weights of edges (i.e., links) connected to a node (i.e., brain region). Increase in weight signifies increase in strength of connections between two nodes and increase in node strength reflects increased functional connections between one node and all other nodes connected to it. The results demonstrate that ECS increases the strength of connections between ROIs acutely after stimulation. This effect is more anteriorly located and highest in M1.

What is the significance of the increase in M1 node strength acutely after ECS? Previous work demonstrates that in the approach to seizure termination, brain electrical activity—as measured through LFP, ECoG, and EEG recordings—exhibit the following dynamical signatures: increased temporal correlation, decreased dominant oscillation frequency, and flickering (i.e., when noise pushes a bistable system back and forth between two alternative

states) (Kramer et al., 2012, Scheffer et al., 2009). The widescale increase in temporal correlation and the slowing of oscillation frequency in the acute post-ictal period after ECS may reflect previously described seizure termination dynamics (Bauer et al., 2017, Jirsa et al., 2014, Kramer et al., 2012) and M1 may play a crucial role in seizure termination.

The primary motor cortex has been known to be involved in the execution of movement—specifically in encoding the force, direction, extent, and speed of movement—by activating specific muscles or muscle groups via the motor neurons in the spinal cord. Additionally, M1 lesions have been demonstrated to result in spasticity (i.e., increased tone) and decrease in power. Interestingly, there is mounting evidence that M1 is involved in negative motor response—a phenomenon wherein electrical stimulation, instead of the typical positive sensorimotor effects (i.e., finger tapping or limb movement), elicits inhibition of ongoing movement (Filevich et al., 2012). In humans, negative motor areas are widely distributed throughout the precentral gyrus and fronto-central cortex and include portions of M1, premotor cortex, and supplementary motor cortex (Borggraefe et al., 2016, Filevich et al, 2012, Ikeda et al., 2000). Mapping analogous negative motor areas in other mammals including rodents would be fertile ground for future research. Seizure termination may involve active inhibition of motor behaviour, instead of a passive absence of encoding for execution of movement, and the increase in strength of functional connection with M1 may facilitate the process of seizure termination by inhibiting ongoing movement.

The cellular mechanisms underlying seizure termination remain nebulous. Mounting evidence reveal dynamical changes during the ictal state that shifts the excitatory-inhibitory balance (Bauer et al., 2017; Ziburkus et al., 2013; Boido et al., 2014). As seizure termination approaches, both excitatory and inhibitory neurons become increasingly active—this may lead to

increased burst activity and longer interburst intervals (Boido et al., 2014). Interneurons receive strong excitatory input, which leads to continuous activation of the inhibitory inputs on pyramidal cells, and seizure termination (Ziburkus et al., 2013). At the synaptic level, Frohlich et al., (2005) demonstrated that dynamic modulation of synaptic transmission can cause termination of paroxysmal activity. Adding that the activity-dependent shift in balance between synaptic excitation and inhibition towards more excitation causes seizure termination by favoring the slow oscillatory state, which permits recovery of baseline extracellular potassium concentration. In addition, they found that slow synaptic depression and change in chloride reversal potential produce similar effects on seizure dynamics.

4.7. RS may mediate therapeutic and adverse cognitive effects after ECT

Default mode hyperconnectivity is one of the most widely reproducible findings in neuropsychiatric disorders such as major depressive disorder and appears promising for translation between humans and animal models as it has been consistently demonstrated across species (Hsu et al., 2016, Stafford et al., 2014, Schwarz et al., 2013, Lu et al., 2012). Though not all components of the default mode system are present in the mouse (Stafford et al., 2014), the retrosplenial cortex is conserved across mammalian species (Gass et al., 2016, Stafford et al., 2014, Vann et al., 2009)—suggesting a key role in DMN function. The significant decrease in node strength in the retrosplenial cortex 24h after ECS may indicate that RS plays a vital role in correcting aberrant hyperconnectivity in pathologic states. Moreover, based on the functions of the retrosplenial cortex, the decrease in strength in this node may play a role in mediating both the major side effect (i.e., memory loss) and therapeutic effect (i.e., antidepressant) of ECT.

Multiple lines of evidence highlight the critical role of the retrosplenial cortex in memory formation and retrieval and its dysfunction has been implicated in symptoms of neuropsychiatric disorders. Anatomically, the retrosplenial cortex has reciprocal links with the hippocampal formation, parahippocampal region, anterior thalamic nuclei, parietal cortex, secondary motor cortex, anterior cingulate, and visual cortex (Powell et al., 2017, Yamawaki et al., 2016, Vann et al., 2009, Shibata et al., 2004). Lesion studies in rodents demonstrate that, in addition to disrupting tests of spatial memory (Miller et al., 2014, Aggleton, 2010, Vann et al., 2009), retrosplenial cortex lesions can impair recency memory (Powell et al., 2017), disrupt a rodent analogue of the Stroop task—i.e., selecting between conflicting responses and inhibit responding to task-irrelevant cues (Nelson et al., 2014) , and impair crossmodal object recognition (Hindley et al., 2014). Moreover, there is substantial behavioural and clinical evidence that the retrosplenial cortex is essential for the formation and retrieval of episodic memory (Todd et al., 2016, 2015, Kwapis et al., 2015, Miller et al., 2014)—which may be due to its role in binding together multiple cues in the environment (Todd et al., 2015). Network analysis in rodent and human imaging studies reveal increased functional coupling between the retrosplenial cortex and anterior cingulate (von Hohenberg et al., 2018; Gass et al., 2016) and insular cortices (Hogeveen et al., 2018) in depression as well as anxiety and depressive symptoms in autism. Specifically, there are evidence showing that increased functional connectivity between the posterior cingulate cortex—which the retrosplenial cortex is part of (Vann et al., 2009)—and the medial prefrontal cortex (i.e., anterior cingulate cortex) is positively correlated with rumination (Kucyi et al., 2014, Berman et al., 2011).

The major side effect of electroconvulsive therapy is the impairment of episodic memories (Bergfeld et al., 2017, Kroes et al., 2014, Lisanby et al., 2000). The widescale decrease

in functional connectivity and the decrease in strength specifically in the retrosplenial cortex provides evidence that the retrosplenial cortex may be involved in alleviating symptoms of disorders such as major depression (i.e., rumination) as well as mediating the unwanted effects of episodic memory loss. The decrease in functional connectivity seen 24h after ECT may serve to correct aberrant hyperconnnectivity in the default mode network in neuropsychiatric disorders such as major depression.

4.8. Caveats and Limitations

GCamp6

Transgenic mouse lines such as GCaMP6 mice are invaluable tools for measuring neural activity with optical imaging. Genetically encoded calcium-sensitive fluorescent proteins present advantages over viral expression or bulk injection: less invasive, more consistent expression level among cells, allows imaging across a wider expanse of the brain, and permits longitudinal imaging due to consistent expression across the subject's lifespan. Steinmetz et al. (2017) report aberrant electrical activity, measured electrophysiologically and with imaging, that resembled interictal spikes some genotypes of transgenic mice expressing GCaMP6. They described the aberrant electrical activity as having: ∼0.1–0.5 Hz rate, very large in amplitude (>1.0 mV local field potentials, >10% df/f widefield imaging signals), brief duration, and typically cover large regions of cortex. The cause of "epileptiform" activity observed in various GCaMP mouse strains may be due to Emx1-Cre expression as transgenics expressing Emx1-Cre, which drives Cre expression in excitatory neurons, have been found to exhibit enhanced seizure susceptibility (Kim et al., 2013). It is also likely due to a combination of factors including Cre toxicity, tTa toxicity, and broad expression of GCaMP, particularly during development (Steinmetz et al., 2017).

The observed "epileptiform" events were most prominent in mice where GCaMP expression was driven by Ai93. In this study, we used the Ai94 line. In their recordings only one Ai94 mouse exhibited aberrant neural activity and they that this does not indicate that all mice of that genotype exhibit them. Moreover, we checked the presence of large amplitude events in control mice from a trace of their mean fluorescence activity and none were found (data not shown). Finally, long LFP recordings by Xiao et al. (2017) demonstrate relatively normal up down states even in Ai93 mice in our colony.

Alternatives have been proposed for the excitatory expression of GCaMP. Namely, Slc17a7-Cre as an alternative to Emx1-Cre for the GCaMP6f sensor and Camk2a-tTA driver with tetO-responsive GCaMP6s for the GCaMP6s sensor (Wekselblatt et al., 2016; Steinmetz et al., 2017).

ECS: auricular electrodes

It is important to note the electrode placement used since it is a crucial determinant of the spread of induced electric field and the relative degree of stimulation of different brain regions (Peterchev et al., 2010). Ear clip electrode is the most commonly used placement (Buel et al., 2017, Bernabei et al., 2014, O'Donovan et al., 2014, Weber et al., 2013)—due to its relative ease of application and the requirement of only one experimenter to apply stimulations (versus two for corneal electrodes). However, a computational model shows that the strongest electric field induced by ear clip electrodes is towards posterior brain regions (i.e., cerebellum and midbrain) (Bernabei et al., 2014), while corneal and cortical electrode placement induces the strongest electric field in frontal brain regions. Despite differences in localization of the strongest electric field between auricular versus corneal or cortical electrode placement, it has been previously shown that they result in similar behavioural and molecular changes. First, both corneal and

auricular ECS induce behavioural seizures of similar duration (Ferraro et al., 1990). Second, cortical (Theilmann et al., 2014), corneal (Lloyd and Sattin, 2015), and auricular (Chang et al., 2017) ECS induce antidepressant-like effect on animal models of depression. Third, both corneal and auricular ECS lead to an increase in GABA levels across many brain regions (Ferraro et al., 1990). ECT has been shown to increase serum GABA levels in humans (Esel et al., 2008).

In sum, auricular electrode placement was used in this study due to: 1) its relative ease of use; 2) the ability for one experimenter to apply stimulations; 3) its non-invasive nature; 4) behavioural changes (i.e., antidepressant-like effect, seizure duration) and 5) molecular changes (i.e., region-specific increase in GABA levels) that are similar to corneal and/or cortical electrode placement.

Fourier analysis

Signals recorded from neurons consist of oscillations that cover a broad frequency spectrum. The most commonly used technique for this spectral decomposition has been the Fourier analysis (Uhlhaas and Singer, 2006). To explore the spectral features of calcium signals, the Fourier transform was processed on the fluorescence images (Vanni et al., 2017, Vanni et al., 2010a,b), which imparts the ability to examine the relative contributions of various frequencies to the overall (calcium) signal (Wallisch et al., 2009). Brain activity associated within each specific frequency band was measured by averaging the power amplitude of Fourier within a frequency window.

The most prominent drawback of the Fourier transform is the assumption that the signal is stationary—indicating that certain statistical properties of the signal is uniform throughout the whole recording (Wallisch et al., 2009). Unfortunately, many biological signals are not

stationary. Neural activity is state-dependent—varying among resting state, motor activity, and differing cognitive demands (Billeke, 2017) as well as changing as a function of sensory input and history of network activity (Nadim et al., 2008). Moreover, spontaneous image recordings in mice do not completely capture resting state functional imaging in humans. Working with humans has the benefit of being able to instruct subjects to refrain from movement during recordings. In mice, this is not possible. Although the head is restrained to allow for optical imaging, mice still move their limbs and whiskers at various points during recordings which effects changes in fluorescence at different timepoints. One way to address this is to separate movement on and off timepoints and analyze them separately.

A more effective analysis for nonstationary signals such as neural oscillatory activity are wavelet-based techniques. The transform is computed for different segments of the signal in the time and in the frequency domain (Quotb et al., 2011). In contrast to the Fourier transform which has a uniform time–frequency distribution, the wavelet transform provides a multi resolution analysis (Daubechies, 1992; Finn and Lopresti, 2003). Hence, it is better suited for analyzing nonstationary signals such as neural oscillations.

4.9. Future Directions

Subcortical and cortical network interactions

It has been hypothesized that, in order for ECT to be effective, seizure activity must reach subcortical structures (Leaver et al., 2016). The involvement of subcortical structures is intuitive since all regions of the cortex have extensive subcortical connections—cortical networks operate as part of a larger, whole brain system (Bressler, 1995). The coordination of activity in various regions has been postulated to depend on cortical and subcortical dynamic control processes

(Van Essen et al., 1994; Bressler et al., 1994; Olshausen et al., 1993). Recent work in our lab demonstrated that thalamic neuronal activity predicts specific cycles of wide-scale cortical inhibition and excitation (Xiao et a., 2017). The thalamus putatively plays a critical role in cortico-cortical interactions and feedback (Guillery and Sherman, 2002). The mediodorsal thalamus has direct anatomical connections with the anterior cingulate cortex, medial prefrontal cortex (as well as the hippocampus) (Ongür and Price, 2000; Ray and Price, 1993). The dorsal anterior cingulate cortex and mediodorsal thalamus have been linked to ECT-related seizure (Leaver et al., 2016) and it has been suggested that thalamo-cortical oscillations might contribute to seizure termination via modulating cortical synchronization (Evangelista et al., 2015). Moreover, the ventral striatal loop and mesolimbic reward pathway have been implicated in ECT response (Leaver et al., 2016; McNally and Blumenfeld, 2004). Simultaneous wide-field GCaMP imaging and sub-cortical cellular electrophysiology (Xiao et a., 2017) offers the ability to investigate relationships between single neuron spiking in subcortical structures, such as the thalamus, and mesoscopic cortical activity during and after ECS.

Depression

Currently, ECT prevails as the most effective treatment for depression with a response rate of 70% to 85.7% (Brakemeier et al., 2013 and Tokutsu et al., 2013). Previous work in our lab demonstrated increased functional connectivity in a mouse model of depression (McGirr et al., 2017). A logical extension of this study and the previous work in our lab is to apply ECS on a depression model and examine whether it can indeed attenuate hyperconnectivity in the depression model. Though it has already been shown in humans that ECT does correct aberrant functional connectivity in depression, doing so in an animal model allows further loss of function and rescue experiments—through optogenetic or chemogenic manipulations—that are not ethical

in human subjects. This offers the opportunity to provide direct evidence of the involvement of functional networks in the antidepressant mechanism of ECT.

Memory

Impairment of episodic memory is the most prominent side effect of ECT (Bergfeld et al., 2017, Kroes et al., 2014, Lisanby et al., 2000). The significant decrease in node strength in the retrosplenial cortex 24h after ECS may indicate that RS plays a vital role in correcting aberrant hyperconnectivity in pathologic states. There is substantial behavioural and clinical evidence that the retrosplenial cortex is essential for the formation and retrieval of episodic memory (Todd et al., 2016, 2015, Kwapis et al., 2015, Miller et al., 2014)—which may be due to its role in binding together multiple cues in the environment (Todd et al., 2015). What is the mechanism of memory loss after ECT? What brain regions are most affected? What changes occur as memories are gradually regained? Optogenetic and chemogenic manipulations offer the ability to provide empirical evidence of the involvement of RS (and other brain regions) in ECT-induced memory impairment and to examine the mechanism of how memories are disrupted and regained after ECT.

Overall conclusions

To our knowledge, this study is the first to achieve longitudinal imaging of neuronal population activity after ECS—with millisecond temporal resolution spanning a broad expanse of cortex using widefield calcium imaging. Utilizing this technique, we have shown that ECS modulates activity both within and between cortical regions.

The combination of changes in power in various frequency bands provides evidence that ECS results in region-specific slowing of cortical activity. This is characterized by increased power in delta (1-4 Hz) and theta (4-7 Hz), together with decreased power in alpha (8-12 Hz). In this study, the regions with the most prominent slowing of neural oscillations are M1, BC, and RS. Previous retrograde, anterograde, and optogenetic photostimulation studies reveal anatomical and functional connections between these and related regions (Yamawaki et al., 2016; Todd and Bucci, 2015; Shibata and Naito, 2008; Mao et al., 2011; Zakiewicz et al., 2014). As the cortico-cortical and the cortico-subcortical connections of these regions have been associated with coupling motor and sensory signals, motor control, and memory (Yamawaki et al., 2016; Mao et al., 2011), this provides support that ECS modulates memory that requires sensorimotor integration such as episodic memory. Impairment of episodic memory is the most prominent side effect of ECT (Bergfeld et al., 2017, Kroes et al., 2014, Lisanby et al., 2000).

This work also shows for the first time that the functional connectivity changes after ECS are dynamic—demonstrating increased correlated activity acutely after stimulation which shifts to decreased co-activation between regions 24 h after. The acute effect of increased temporal correlation combined with slowing of neural oscillations recapitulates previously described seizure termination dynamics (Bauer et al., 2017, Jirsa et al., 2014, Kramer et al., 2012). This study reveals that M1 has the greatest increase in node strength acutely after ECS, which

suggests that it may play a crucial role in seizure termination. The 24h effect demonstrating a widescale decrease in functional connectivity, in addition to the greatest decrease in strength seen specifically in the retrosplenial cortex provides evidence that the retrosplenial cortex may mediate both therapeutic (i.e., decreased rumination) and adverse (i.e., episodic memory loss) cognitive effects after ECT.

Elucidating the region-specific effects in activity and the time-dependent changes in functional connectivity after ECS may provide opportunities to further dissect the mechanisms of the therapeutic and adverse effects of ECT.

References

Journal articles

Aggleton J.P. Understanding retrosplenial amnesia: insights from animal studies. (2010). Neuropsychologia.;48:2328–2338

Alper KR, John ER, Brodie J, Gunther W, Daruwala R, Prichep LS. (2006). Correlation of PET and qEEG in normal subjects. Psychiatry Research.;146(3):271–282. doi: 10.1016/j.pscychresns.2005.06.008.

Andrade C (2010). Dose calculation with brief-pulse ECT demystified. Indian J Psychiatry.;52(3):276-8. doi: 10.4103/0019-5545.70995.

Baghai TC[1], Möller HJ. (2008). Electroconvulsive therapy and its different indications. Dialogues Clin Neurosci.;10(1):105-17.

Bai S, Loo C, Al Abed A, Dokos S. (2012). A computational model of direct brain excitation induced by electroconvulsive therapy: comparison among three conventional electrode placements. Brain Stimul. ;5(3):408-421. doi: 10.1016/j.brs.2011.07.004. Epub 2011 Aug 9.

Bailine SH, Rifkin A, Kayne E, Selzer JA, Vital-Herne J, Blieka M, Pollack S. (2000). Comparison of bifrontal and bitemporal ECT for major depression. Am J Psychiatry.;157(1):121-3.

Bajbouj M, Luborzewski A, Danker-Hopfe H, Lang UE.(2005). Motor cortical excitability in depressive patients after electroconvulsive therapy and repetitive transcranial magnetic stimulation. J ECT. ;21:243–245. doi: 10.1097/01.yct.0000180039.12176.9c.

Bartos, M., Manor, Y., Nadim, F., Marder, E. & Nusbaum, M. P. 1999) *Coordination of fast and slow rhythmic neuronal circuits*. J. Neurosci. **19**, 6650–6660

Barttfeld P, Uhrig L, Sitt JD, Sigman M, Jarraya B, Dehaene S (2015). Signature of consciousness in the dynamics of resting-state brain activity. Proc. Natl. Acad. Sci. U.S.A., 112(3):887-92. doi: 10.1073/pnas.1418031112.

Bauer P et al. (2017). Dynamics of convulsive seizure termination and postictal generalized EEG suppression. Brain. ;140(3):655-668. doi: 10.1093/brain/aww322.

Beall EB, Malone DA, Dale RM, Muzina DJ, Koenig KA, Bhattacharrya PK, Jones SE, Phillips MD, Lowe MJ. (2012). Effects of electroconvulsive therapy on brain functional activation and connectivity in depression. J ECT. 2012 Dec;28(4):234-41. doi: 10.1097/YCT.0b013e31825ebcc7

Bergfeld IO et al (2017). Episodic memory following deep brain stimulation of the ventral anterior limb of the internal capsule and electroconvulsive therapy. Brain Stimul. 2017 Sep - Oct;10(5):959-966. doi: 10.1016/j.brs.2017.07.006. Epub 2017 Jul 19.

Bernabei JM, Lee WH, Peterchev AV. (2014). Modeling transcranial electric stimulation in mouse: a high resolution finite element study. Conf Proc IEEE Eng Med Biol Soc.:406-9. doi: 10.1109/EMBC.2014.6943614.

Billeke P et al. (2017). Brain state-dependent recruitment of high-frequency oscillations in the human hippocampus. Cortex. 2017 Sep;94:87-99. doi: 10.1016/j.cortex.2017.06.002. Epub 2017 Jun 23.

Boido D, Gnatkovsky V, Uva L, Francione S, de Curtis M.(2014). Simultaneous enhancement of excitation and postburst inhibition at the end of focal seizures. Ann Neurol ; 76: 826–36.

Bonnefond M, Jensen O.(2013). The role of gamma and alpha oscillations for blocking out distraction. Commun Integr Biol. ;6(1):e22702. doi: 10.4161/cib.22702.

Borggraefe I, Catarino CB, Rémi J, Vollmar C^2, Peraud A, Winkler PA, Noachtar S. Lateralization of cortical negative motor areas. (2016). Clin Neurophysiol. ;127(10):3314-21. doi: 10.1016/j.clinph.2016.08.001. Epub 2016 Aug 10.

Boroojerdi B, Meister IG, Foltys H, Sparing R, Cohen LG, Töpper R. (2002). Visual and motor cortex excitability: a transcranial magnetic stimulation study. Clin Neurophysiol. ;113:1501–1504. doi: 10.1016/S1388-2457(02)00198-0

Bressler SL (1995). Large-scale cortical networks and cognition. Brain Res Brain Res Rev. 1995 Mar;20(3):288-304.

Buzsaki G, Draguhn A. (2004). Neuronal oscillations in cortical networks. Science. ;304:1926–1929.

Cano M et al. (2016). Modulation of Limbic and Prefrontal Connectivity by Electroconvulsive Therapy in Treatment-resistant Depression: A Preliminary Study. Brain Stimul.;9(1):65-71. doi: 10.1016/j.brs.2015.08.016.

Casarotto S, Canali P, Rosanova M, Pigorini A, Fecchio M, Mariotti M, Lucca A, Colombo C, Benedetti F, Massimini M. (2013). Assessing the effects of electroconvulsive therapy on cortical excitability by means of transcranial magnetic stimulation and electroencephalography. Brain Topogr. ;26(2):326-37. doi: 10.1007/s10548-012-0256-8. Epub 2012 Oct 9.

Chang AD et al. (2017). Narp Mediates Antidepressant-Like Effects of Electroconvulsive Seizures. Neuropsychopharmacology. 2018 Apr;43(5):1088-1098. doi: 10.1038/npp.2017.252. Epub 2017 Oct 20.

Chen AC, Feng W, Zhao H, Yin Y, Wang P. (2008). EEG default mode network in the human brain: spectral regional field powers. Neuroimage. ;41(2):561–574. doi: 10.1016/j.neuroimage.2007.12.064.

Chen TW, Wardill TJ, Sun Y, Pulver SR, Renninger SL, Baohan A, Schreiter ER, Kerr RA, Orger MB, Jayaraman V, Looger LL, Svoboda K, Kim DS (2013) Ultrasensitive fluorescent proteins for imaging neuronal activity. Nature 499:295–300. doi:10.1038/nature12354 pmid:23868258

Chistyakov AV, Kaplan B, Rubichek O, Kreinin I, Koren D, Hafner H, Feinsod M, Klein E.(2005). Effect of electroconvulsive therapy on cortical excitability in patients with major depression: a transcranial magnetic stimulation study. Clin Neurophysiol. ;116:386–392. doi: 10.1016/j.clinph.2004.09.008.

Chung S, Kim HJ, Yoon IS, Kim HJ, Choi SH, Kim YS, Shin KH. (2013). Electroconvulsive shock increases SIRT1 immunoreactivity in the mouse hippocampus and hypothalamus. J ECT. ;29(2):93-100. doi: 10.1097/YCT.0b013e31827659f7.

Ciobanu L, Reynaud O, Uhrig L, Jarraya B, Le Bihan D. (2012). Effects of anesthetic agents on brain blood oxygenation level revealed with ultra-high field MRI. PLoS One.;7(3):e32645. doi: 10.1371/journal.pone.0032645

Cycowicz YM, Luber B, Spellman T, Lisanby SH. (2008). Differential neurophysiological effects of magnetic seizure therapy (MST) and electroconvulsiveshock (ECS) in non-human primates. Clin EEG Neurosci. 2008 Jul;39(3):144-9.

Datta A[1], Elwassif M, Battaglia F, Bikson M. (2008). Transcranial current stimulation focality using disc and ring electrode configurations: FEM analysis. J Neural Eng. Jun;5(2):163-74. doi: 10.1088/1741-2560/5/2/007.

Delva NJ, Brunet D, Hawken ER, Kesteven RM, Lawson JS, Lywood DW, Rodenburg M, Waldron JJ. (2000) Electrical dose and seizure threshold: relations to clinical outcome and cognitive effects in bifrontal, bitemporal, and right unilateral ECT. J ECT.;16(4):361-9.

Deng ZD, Lisanby SH, Peterchev AV.(2011). Electric field strength and focality in electroconvulsive therapy and magnetic seizure therapy: a finite element simulation study. J Neural Eng.;8(1):016007. doi: 10.1088/1741-2560/8/1/016007. Epub 2011 Jan 19.

Devanand DP, Lisanby SH, Nobler MS, et al. (1998). The relative efficiency of altering pulse frequency or train duration when determining seizure threshold. J ECT.;14:227–235.

Ekstrom AD, Watrous AJ (2013) Multifaceted roles for low-frequency oscillations in bottom-up and top-down processing during navigation and memory. Neuroimage. ;85 Pt 2:667-77. doi: 10.1016/j.neuroimage.2013.06.049. Epub 2013 Jun 20.

Enev M, McNally KA, Varghese G, Zubal IG, Ostroff RB, Blumenfeld H. (2007). Imaging onset and propagation of ECT-induced seizures. Epilepsia. ;48(2):238-44.

Eranti SV, McLoughlin DM. (2003) Electroconvulsive therapy—state of the art. Br. J. Psychiatry.;182:8–9.

Esel E, Kose K, Hacimusalar Y, Ozsoy S, Kula M, Candan Z, Turan T.(2008). The effects of electroconvulsive therapy on GABAergic function in major depressive patients. J ECT. 2008 Sep;24(3):224-8. oi: 10.1097/YCT.0b013e31815cbaa1.

Ferraro TN, Golden GT, Hare TA. (1990). Repeated Electroconvulsive Shock Selectively Alters gamma-Aminobutyric Acid Levels in the Rat Brain: Effect of Electrode Placement. Convuls Ther. ;6(3):199-208.

Filevich E, Kühn S, Haggard P. (2012). Negative motor phenomena in cortical stimulation: implications for inhibitory control of human action. Cortex. ;48(10):1251-61. doi: 10.1016/j.cortex.2012.04.014. Epub 2012 May 7.

Fink M. EEG changes with antipsychotic drugs. Am J Psychiatry (2002) 159:1439 discussion 1439.10.1176/appi.ajp.159.8.1439

Folkerts H. The ictal electroencephalogram as a marker for the efficacy of electroconvulsive therapy. Eur Arch Psychiatry Clin Neurosci. 1996;246:155–164. doi: 10.1007/BF02189117.

Fontenelle LF, Coutinho ES, Lins-Martins NM, Fitzgerald PB, Fujiwara H, Yücel M. (2015). Electroconvulsive therapy for obsessive-compulsive disorder: a systematic review. J Clin Psychiatry.;76(7):949-57. doi: 10.4088/JCP.14r09129.

Fries, P., Reynolds, J., Rorie, A.& Desimone, R. (2001(. *Modulation ofoscillatory neuronal synchronization by selective visual attention*. Science **291**, 1560–1563

Fröhlich F, Bazhenov M, Timofeev I, Sejnowski TJ.(2005). Maintenance and termination of neocortical oscillations by dynamic modulation of intrinsic and synaptic excitability. Thalamus Relat Syst. ;3(2):147-156.

Gass N et al (2016). Brain network reorganization differs in response to stress in rats genetically predisposed to depression and stress-resilient rats. Transl Psychiatry. ;6(12):e970. doi: 10.1038/tp.2016.233.

Gerner RH, Hare TA (1981) CSF GABA in normal subjects and patients with depression, schizophrenia, mania, and anorexia nervosa. Am J Psychiatry.; 138(8):1098-101.

Gerwig M, Kastrup O, Meyer B-U, Niehaus L. (2003). Evaluation of cortical excitability by motor and phosphene thresholds in transcranial magnetic stimulation. J Neurol Sci. ;215:75–78. doi: 10.1016/S0022-510X(03)00228-4.

Gitlin M (2006). Treatment-resistant bipolar disorder. Mol Psychiatry. 2006 Mar;11(3):227-40.

Griffiths KM[1], Carron-Arthur B, Parsons A, Reid R. (2014). Effectiveness of programs for reducing the stigma associated with mental disorders. A meta-analysis of randomized controlled trials. World Psychiatry. 2014 Jun;13(2):161-75. doi: 10.1002/wps.20129.

Grienberger C, Konnerth A. (2012). Imaging calcium in neurons. Neuron. 2012 Mar 8;73(5):862-85. doi: 10.1016/j.neuron.2012.02.011.

Guillery RW, Sherman SM (2002). Thalamic relay functions and their role in corticocortical communication: generalizations from the visual system. Neuron. 33(2):163-75.

Hamilton C, Ma Y, Zhang N. (2017). Global reduction of information exchange during anesthetic-induced unconsciousness. Brain Struct Funct.;222(7):3205-3216. doi: 10.1007/s00429-017-1396-0. Epub 2017 Mar 13.

Hemphill KE, Walter WG. (1941). The treatment of mental disorders by electrically induced convulsions. J. Ment. Sci. ;87:256–275.

Hillman EM (2014). Coupling mechanism and significance of the BOLD signal: a status report. Annu Rev Neurosci. 2014;37:161-81. doi: 10.1146/annurev-neuro-071013-014111.

Hindley E.L., Nelson A.J.D., Aggleton J.P., Vann S.D. (2014). Dysgranular retrosplenial cortex lesions in rats disrupt cross-modal object recognition. Learn. Mem. (Cold Spring Harb. N.Y.) ;21:171–179.

Hlinka J, Alexakis C, Diukova A, Liddle PF, Auer DP. (2010). Slow EEG pattern predicts reduced intrinsic functional connectivity in the default mode network: an inter-subject analysis. Neuroimage. ;53(1):239-46. doi: 10.1016/j.neuroimage.2010.06.002. Epub 2010 Jun 9.

Hogeveen J, Krug MK, Elliott MV, Solomon M. (2018). Insula-Retrosplenial Cortex Overconnectivity Increases Internalizing via Reduced Insight in Autism. Biol Psychiatry. ;84(4):287-294. doi: 10.1016/j.biopsych.2018.01.015. Epub 2018 Jan 31.

Ikeda A, Ohara S, Matsumoto R, Kunieda T, Nagamine T, Miyamoto S, Kohara N, Taki W, Hashimoto N, Shibasaki H. (2000) Role of primary sensorimotor cortices in generating inhibitory motor response in humans. Brain. ;123 (Pt 8):1710-21.

Jirsa VK, Stacey WC, Quilichini PP, Ivanov AI, Bernard C. (2014). On the nature of seizure dynamics. Brain. ;137(Pt 8):2210-30. doi: 10.1093/brain/awu133. Epub 2014 Jun 11.

Jonckers E, Delgado y Palacios R, Shah D, Guglielmetti C, Verhoye M, Van der Linden A. (2014). Different anesthesia regimes modulate the functional connectivity outcome in mice. Magn Reson Med. 2014 Oct;72(4):1103-12. doi: 10.1002/mrm.24990. Epub 2013 Oct 29.

Kaiser, R.,Andrews-Hanna, J., Wagner, T., Pizzagalli, D. (2015). Large-Scale Network Dysfunction in Major Depressive Disorder: A Meta-analysis of Resting-State Functional Connectivity. *JAMA Psychiatry.* 2015;72(6):603-611. doi:10.1001/jamapsychiatry.2015.0071

Khalid, A., Kim, B., Chung, M., Ye, J., Jeon, D. (2014). Tracing the evolution of multi-scale functional networks in a mouse model of depression using persistent brain network homology. *NeuroImage*. 101 (2014) 351–363

Kellner CH et al (2005). Relief of expressed suicidal intent by ECT: a consortium for research in ECT study. Am J Psychiatry.;162(5):977-82.

Kennedy R, Mittal D, O'Jile J. Electroconvulsive therapy in movement disorders: an update. *J Neuropsychiatry Clin Neurosci* 2003;15:407-21.

Kerner N, Prudic J. (2014). Current electroconvulsive therapy practice and research in the geriatric population. Neuropsychiatry (London).;4(1):33-54.

Kessler RC, Berglund P, Demler O, Jin R, Merikangas KR, Walters EE. (2005). Lifetime prevalence and age-of-onset distributions of DSM-IV disorders in the National Comorbidity Survey Replication. Arch Gen Psychiatry. ;62(6):593-602.

Kibret B, Premaratne M, Sullivan C, Thomson RH, Fitzgerald PB (2018). Electroconvulsive therapy (ECT) during pregnancy: quantifying and assessing the electric field strength inside the foetal brain.;8(1):4128. doi: 10.1038/s41598-018-22528-x.

Klimesch W, Sauseng P, Hanslmayr S.(2007). EEG alpha oscillations: the inhibition-timing hypothesis. Brain Res Rev. ;53(1):63-88. Epub 2006 Aug 1.

Knyazev GG (2007) Motivation, emotion, and their inhibitory control mirrored in brain oscillations. Neurosci Biobehav Rev 31: 377–395.

Kopell, N., Ermentrout, G. B., Whittington, M. A. & Traub, R. D. (2000). *Gamma rhythms and beta rhythms have different synchronization properties*. Proc. Natl Acad. Sci. USA **97**, 1867–1872

Kramer MA et al. (2012). Human seizures self-terminate across spatial scales via a critical transition. Proc Natl Acad Sci U S A. ;109(51):21116-21. doi: 10.1073/pnas.1210047110. Epub 2012 Dec 4.

Kroes MC et al. (2014). An electroconvulsive therapy procedure impairs reconsolidation of episodic memories in humans. Nat Neurosci. 2014 Feb;17(2):204-6. doi: 10.1038/nn.3609. Epub 2013 Dec 22.

Kucyi A, Moayedi M, Weissman-Fogel I, Goldberg MB, Freeman BV, Tenenbaum HC, Davis KD.(2014). Enhanced medial prefrontal-default mode network functional connectivity in chronic pain and its association with pain rumination. J Neurosci. ;34(11):3969-75. doi: 10.1523/JNEUROSCI.5055-13.2014.

Leaver et al. (2016). Modulation of intrinsic brain activity by electroconvulsive therapy in major depression. Biol Psychiatry Cogn Neurosci Neuroimaging. 2016 Jan; 1(1): 77–86. doi: 10.1016/j.bpsc.2015.09.001

Lee WH, Deng ZD, Kim TS, Laine AF, Lisanby SH, Peterchev AV. (2016). Comparison of electric field strength and spatial distribution of electroconvulsive therapy and magnetic seizure therapy in a realistic human head model. Neuroimage.;59(3):2110-23. doi: 10.1016/j.neuroimage.2011.10.029. Epub 2011 Oct 18.

Leiknes KA, Jarosh-von Schweder L, Høie B. (2012) Contemporary use and practice of electroconvulsive therapy worldwide .Brain Behav. ;2(3):283-344. doi: 10.1002/brb3.37.

Liang Z, Liu X, Zhang N. (2015). Dynamic resting state functional connectivity in awake and anesthetized rodents. Neuroimage.;104:89-99. doi: 10.1016/j.neuroimage.2014.10.013. Epub 2014 Oct 12.

Lisanby SH, Belmaker RH. (2000). Animal models of the mechanisms of action of repetitive transcranial magnetic stimulation(RTMS): comparisons with electroconvulsive shock (ECS). Depress Anxiety. 2000;12(3):178-87.

Liu et al. (2014). Electroconvulsive Therapy on Severe Obsessive-Compulsive Disorder Comorbid Depressive Symptoms. Psychiatry Investig.; 11(2): 210–213.

Lloyd RL, Sattin A. (2015). The Behavioral Physiology and Antidepressant Mechanisms of Electroconvulsive Shock. J ECT. ;31(3):159-66. doi: 10.1097/YCT.0000000000000195.

Lunde ME, Lee EK, Rasmussen KG (2006). Electroconvulsive therapy in patients with epilepsy. Epilepsy Behav.;9(2):355-9. Epub 2006 Jul 28.

Luscher B, Shen Q, Sahir N. (2011). The GABAergic deficit hypothesis of major depressive disorder. Mol Psychiatry.;16(4):383-406. doi: 10.1038/mp.2010.120.

Ma Y, Shaik MA, Kim SH, Kozberg MG, Thibodeaux DN, Zhao HT, Yu H, Hillman EMC.(2016). Wide-field optical mapping of neural activity and brain haemodynamics:

considerations and novel approaches. Philosophical Transactions of the Royal Society B: Biological Sciences. ;371:20150360 doi: 10.1098/rstb.2015.0360.

Ma Y, Hamilton C, Zhang N. (2017). Dynamic Connectivity Patterns in Conscious and Unconscious Brain. Brain Connect. ;7(1):1-12. doi: 10.1089/brain.2016.0464. Epub 2016 Dec 15.

Madisen et al. (2015). Transgenic mice for intersectional targeting of neural sensors and effectors with high specificity and performance. Neuron. ;85:942–958. doi: 10.1016/j.neuron.2015.02.022.

Malonek D, Grinvald A. (1996). Interactions between electrical activity and cortical microcirculation revealed by imaging spectroscopy: implications for functional brain mapping. Science. 1996 Apr 26;272(5261):551-4.

Mantini D, Perrucci MG, Del Gratta C, Romani GL, Corbetta M.(2007). Electrophysiological signatures of resting state networks in the human brain. Proc Natl Acad Sci U S A. 2007 Aug 7;104(32):13170-5. Epub 2007 Aug 1.

Mao T, Kusefoglu D, Hooks BM, Huber D, Petreanu L, Svoboda K. (2011). Long-range neuronal circuits underlying the interaction between sensory and motor cortex. Neuron. ;72(1):111-23. doi: 10.1016/j.neuron.2011.07.029.

McNally KA and Blumenfeld H (2004). Focal network involvement in generalized seizures: new insights from electroconvulsive therapy. Epilepsy Behav; 5(1): 3-12.

Miller A.M.P., Vedder L.C., Law L.M., Smith D.M. (2014). Cues, context, and long-term memory: the role of the retrosplenial cortex in spatial cognition. Front. Hum. Neurosci. ; ;8:586. doi: 10.3389/fnhum.2014.00586. eCollection 2014.

Mohajerani MH, Chan AW, Mohsenvand M, LeDue J, Liu R, McVea DA, Boyd JD, Wang YT, Reimers M, Murphy TH (2013) Spontaneous cortical activity alternates between motifs defined by regional axonal projections. Nat Neurosci 16:1426–1435. doi:10.1038/nn.3499 pmid:23974708

McCall WV. (2001). Electroconvulsive therapy in the era of modern psychopharmacology. *int J Neuropsychopharmacol.* ;4:315–324.

McCormick LM, Yamada T, Yeh M, Brumm MC, Thatcher RW. Antipsychotic effect of electroconvulsive therapy is related to normalization of subgenual cingulate theta activity in psychotic depression. J Psychiatr Res. 2009;43:553–560. doi: 10.1016/j.jpsychires.2008.08.004

McGirr A, LeDue J, Chan AW, Xie Y, Murphy TH. (2017). Cortical functional hyperconnectivity in a mouse model of depression and selective network effects of ketamine. Brain. 2017 Aug 1;140(8):2210-2225. doi: 10.1093/brain/awx142.

Nadim F, Brezina V, Destexhe A, Linster C. (2008). State dependence of network output: modeling and experiments. J Neurosci. ;28(46):11806-13. doi: 10.1523/JNEUROSCI.3796-08.2008.

Nelson AJ, Hindley EL, Haddon JE, Vann SD, Aggleton JP. (2014). A novel role for the rat retrosplenial cortex in cognitive control. Learn Mem. ;21(2):90-7. doi: 10.1101/lm.032136.113.

O'Donovan SM, O'Mara S, Dunn MJ, McLoughlin DM. (2014). The persisting effects of electroconvulsive stimulation on the hippocampal proteome. Brain Res.;1593:106-16. doi: 10.1016/j.brainres.2014.10.020. Epub 2014 Oct 22.

Paasonen J, Stenroos P, Salo RA, Kiviniemi V, Gröhn O. (2018). Functional connectivity under six anesthesia protocols and the awake condition in rat brain. Neuroimage. ;172:9-20. doi: 10.1016/j.neuroimage.2018.01.014. Epub 2018 Jan 28.

Perrin JS, Merz S, Bennett DM, Currie J, Steele DJ, Reid IC, Schwarzbauer C. (2012). Electroconvulsive therapy reduces frontal cortical connectivity in severe depressive disorder. Proc Natl Acad Sci U S A. 2012 Apr 3;109(14):5464-8. doi: 10.1073/pnas.1117206109. Epub 2012 Mar 19.

Perugi et al. (2017). The Role of Electroconvulsive Therapy (ECT) in Bipolar Disorder: Effectiveness in 522 Patients with Bipolar Depression, Mixed-state, Mania and Catatonic Features. Curr Neuropharmacol. 2017 Apr; 15(3): 359–371.

Peterchev AV[1], Rosa MA, Deng ZD, Prudic J, Lisanby SH (2010) Electroconvulsive therapy stimulus parameters: rethinking dosage. J ECT Sep;26(3):159-74. doi: 10.1097/YCT.0b013e3181e48165.

Petrides G[1], Fink M, Husain MM, Knapp RG, Rush AJ, Mueller M, Rummans TA, O'Connor KM, Rasmussen KG Jr, Bernstein HJ, Biggs M, Bailine SH, Kellner CH.

Petrides et al. (2001). ECT remission rates in psychotic versus nonpsychotic depressed patients: a report from CORE. J ECT.;17(4):244-53.

Quotb A, Bornat Y, Renaud S. (2011). Wavelet transform for real-time detection of action potentials in neural signals. Front Neuroeng. ;4:7. doi: 10.3389/fneng.2011.00007. eCollection 2011.

Rosch RE, Hunter PR, Baldeweg T, Friston KJ, Meyer MP. (2018). Calcium imaging and dynamic causal modelling reveal brain-wide changes in effectiveconnectivity and synaptic dynamics during epileptic seizures. PLoS Comput Biol.;14(8):e1006375. doi: 10.1371/journal.pcbi.1006375

Rothschild A (2013). Challenges in the Treatment of Major Depressive Disorder With Psychotic Features. Schizophr Bull.; 39(4): 787–796.

Petty F, Sherman AD (1984). Plasma GABA levels in psychiatric illness. J Affect Disord.; 6(2):131-8.

Powell AL, Nelson AJD, Hindley E, Davies M, Aggleton JP, Vann SD (2017). The rat retrosplenial cortex as a link for frontal functions: A lesion analysis. Behav Brain Res. 29;335:88-102. doi: 10.1016/j.bbr.2017.08.010. Epub 2017 Aug 8.

Sackeim HA, Luber B, Katzman GP, Moeller JR, Prudic J, Devanand DP, Nobler MS.(1996). The effects of electroconvulsive therapy on quantitative electroencephalograms. Relationship to clinical outcome. Arch Gen Psychiatry.;53(9):814-24.

Sakaida M, Sukeno M, Imoto Y, Tsuchiya S, Sugimoto Y, Okuno Y, Segi-Nishida E. (2013). Electroconvulsive seizure-induced changes in gene expression in the mouse hypothalamic paraventricular nucleus. J Psychopharmacol. ;27(11):1058-69. doi: 10.1177/0269881113497612. Epub 2013 Jul 17.

Shibata H, Naito J. (2008). Organization of anterior cingulate and frontal cortical projections to the retrosplenial cortex in the rat. J Comp Neurol. ;506(1):30-45.

Sirotin YB, Das A.(2010). Spatial relationship between flavoprotein fluorescence and the hemodynamic response in the primary visual cortex of alert macaque monkeys. Frontiers in Neuroenergetics.;2:6 doi: 10.3389/fnene.2010.00006.

Sommer M, Dieterich A, Rüther E, Paulus W, Wiltfang J. (2002). Increased transcranial magnetic motor threshold after ECT. A case report. Eur Arch Psychiatry Clin Neurosci. ;252:250–252. doi: 10.1007/s00406-002-0387-0.

Stafford JM et al. (2014). Large-scale topology and the default mode network in the mouse connectome. Proc Natl Acad Sci U S A. ;111(52):18745-50. doi: 10.1073/pnas.1404346111. Epub 2014 Dec 15.

Steinmetz NA et al. (2017). Aberrant Cortical Activity in Multiple GCaMP6-Expressing Transgenic Mouse Lines. eNeuro. 2017 Sep 6;4(5). pii: ENEURO.0207-17.2017. doi: 10.1523/ENEURO.0207-17.2017. eCollection 2017 Sep-Oct.

Steriade M, McCormick DA, Sejnowski TJ (1993) Thalamocortical oscillations in the sleeping and aroused brain. Science 262: 679–685.

Stewart LM, Walsh V, Rothwell JC. (2001). Motor and phosphene thresholds: a transcranial magnetic stimulation correlation study. Neuropsychologia.;39:415–419. doi: 10.1016/S0028-3932(00)00130-5.

Xiao D, Vanni MP, Mitelut CC, Chan AW, LeDue JM, Xie Y, Chen AC, Swindale NV, Murphy TH. (2017). Mapping cortical mesoscopic networks of single spiking cortical or sub-cortical neurons. Elife.;6. pii: e19976. doi: 10.7554/eLife.19976.

Silasi G, Xiao D, Vanni MP, Chen AC, Murphy TH. (2016). Intact skull chronic windows for mesoscopic wide-field imaging in awake mice. J Neurosci Methods. 2016 Jul 15;267:141-9. doi: 10.1016/j.jneumeth.2016.04.012. Epub 2016 Apr 19.

Singh A, Kar SK. (2017). How Electroconvulsive Therapy Works?: Understanding the Neurobiological Mechanisms. Clin Psychopharmacol Neurosci. 2017 Aug 31;15(3):210-221. doi: 10.9758/cpn.2017.15.3.210.

Strassnig M, Riedel M, Müller N. (2004). Electroconvulsive therapy in a patient with Tourette's syndrome and co-morbid Obsessive Compulsive Disorder. World J Biol Psychiatry.;5(3):164-6.

Strome EM, Zis AP, Doudet DJ.(2007). Electroconvulsive shock enhances striatal D1 and D3 receptor binding and improves motor performance in 6-OHDA lesioned rats. J Psychiatry Neurosci. ;32:193–202.

Swartz CM[1], Nelson AI. (2005) Rational electroconvulsive therapy electrode placement. Psychiatrt (Edgmont). Jul;2(7):37-43.

Theilmann W, Löscher W, Socala K, Frieling H, Bleich S, Brandt C. (2014). A new method to model electroconvulsive therapy in rats with increased construct validity and enhanced translational value. J Psychiatr Res.;53:94-8. doi: 10.1016/j.jpsychires.2014.02.007.

Tian L, Hires SA, Mao T, Huber D, Chiappe ME, Chalasani SH, Petreanu L, Akerboom J, McKinney SA, Schreiter ER, Bargmann CI, Jayaraman V, Svoboda K, Looger LL (2009) Imaging neural activity in worms, flies and mice with improved GCaMP calcium indicators. Nat Methods 6:875–881. doi:10.1038/nmeth.1398 pmid:19898485

Todd TP, Bucci DJ. (2015). Retrosplenial Cortex and Long-Term Memory: Molecules to Behavior.Neural Plast.;2015:414173. doi: 10.1155/2015/414173. Epub 2015 Aug 25.

Uhlén P (2004). Spectral analysis of calcium oscillations. Sci STKE. 2004 Nov 9;2004(258):pl15.

Uhlhaas PJ, Singer W.(2006). Neural synchrony in brain disorders: relevance for cognitive dysfunctions and pathophysiology. Neuron. 2006 Oct 5;52(1):155-68.

Vann SD, Aggleton JP, Maguire EA. (2009). What does the retrosplenial cortex do? Nat Rev Neurosci. ;10(11):792-802. doi: 10.1038/nrn2733. Epub 2009 Oct 8.

Vanni MP, Murphy TH. (2014). Mesoscale transcranial spontaneous activity mapping in GCaMP3 transgenic mice reveals extensive reciprocal connections between areas of somatomotor cortex. J Neurosci. 2014 Nov 26;34(48):15931-46. doi: 10.1523/JNEUROSCI.1818-14.2014.

Vanni MP, Chan AW, Balbi M, Silasi G, Murphy TH. (2017). Mesoscale Mapping of Mouse Cortex Reveals Frequency-Dependent Cycling between Distinct Macroscale Functional Modules. J Neurosci.;37(31):7513-7533. doi: 10.1523/JNEUROSCI.3560-16.2017. Epub 2017 Jul 3.

Van Buel et al.(2017). Mouse repeated electroconvulsive seizure (ECS) does not reverse social stress effects but does induce behavioral and hippocampal changes relevant to electroconvulsive therapy (ECT) side-effects in the treatment of depression. PLoS One.;12(9):e0184603. doi: 10.1371/journal.pone.0184603. eCollection 2017

Varela F, Lachaux JP, Rodriguez E, Martinerie J.(2001). The brainweb: phase synchronization and large-scale integration. Nat Rev Neurosci. ;2(4):229-39.

von Stein, A., Chiang, C. & Konig, P. (2000).*Top-down processing mediated by interareal synchronization*. Proc. Natl Acad. Sci. USA **97**, 14748–14753

Wang J, Wei Q, Yuan X, Jiang X, Xu J, Zhou X, Tian Y, Wang K. (2018). Local functional connectivity density is closely associated with the response of electroconvulsive therapy in major depressive disorder. J Affect Disord. ;225:658-664. doi: 10.1016/j.jad.2017.09.001.

Weber T, Baier V, Lentz K, Herrmann E, Krumm B, Sartorius A, Kronenberg G, Bartsch D. (2013). Genetic fate mapping of type-1 stem cell-dependent increase in newborn hippocampal neurons after electroconvulsive seizures. Hippocampus.;23(12):1321-30. doi: 10.1002/hipo.22171. Epub 2013 Sep 2.

Wekselblatt JB, Flister ED, Piscopo DM, Niell CM (2016) Large-scale imaging of cortical dynamics during sensory perception and behavior. J Neurophysiol 115:2852–2866. 10.1152/jn.01056.2015

White BR, Bauer AQ, Snyder AZ, Schlaggar BL, Lee JM, Culver JP (2011) Imaging of functional connectivity in the mouse brain. PLoS One 6:e16322. doi:10.1371/journal.pone.0016322 pmid:21283729

World Health Organization. (2018). Depression. Retrieved from http://www.who.int/news-room/fact-sheets/detail/depression

Yamawaki N, Radulovic J, Shepherd GM. (2016). A Corticocortical Circuit Directly Links Retrosplenial Cortex to M2 in the Mouse. J Neurosci. ;36(36):9365-74. doi: 10.1523/JNEUROSCI.1099-16.2016.

Yoder EJ (2002) In Vivo Microscopy of the Mouse Brain Using Multiphoton Laser Scanning Techniques. Proc SPIE Int Soc Opt Eng. 2002 Jun 17;4620:14-29.

Zakiewicz IM, Bjaalie JG, Leergaard TB. (2014). Brain-wide map of efferent projections from rat barrel cortex. Front Neuroinform.;8:5. doi: 10.3389/fninf.2014.00005. eCollection 2014.

Zhao L, Jiang Y, Zhang H. (2016). Effects of modified electroconvulsive therapy on the electroencephalogram of schizophrenia patients. Springerplus. 12;5(1):1063. doi: 10.1186/s40064-016-2747-7. eCollection 2016.

Žiburkus J, Cressman JR, Schiff SJ. (2013). Seizures as imbalanced up states: excitatory and inhibitory conductances during seizure-like events. J Neurophysiol ; 109: 1296–306.

Books

Bromfield EB, Cavazos JE, Sirven JI, (2006). An Introduction to Epilepsy [Internet]. West Hartford (CT): American Epilepsy Society; Chapter 1, Basic Mechanisms Underlying Seizures and Epilepsy.Available from: https://www.ncbi.nlm.nih.gov/books/NBK2510/

Lyons R (2010). Understanding Digital Signal Processing (3rd Edition). Ann Arbor, Michigan: Pearson Education, Inc

Scheffer M. Critical Transitions in Nature and Society. Princeton, NJ: Princeton Univ Press; 2009.

Wallisch et al. (2009). MATLAB for Neuroscientists. 1st ed. California: Elsevier

Weiner RD., Coffey CE., Folk J., Fochtmann LJ., Greenberg RM., et al. (2001). American Psychiatrie Association Committee on Electroconvulsive Therapy, *The Practice of Electroconvulsive Therapy.* 2nd ed. Washington, DC: American Psychiatric Association